Air mass origin and local impacts ~~Effects~~ on Antarctic snow isotopic composition: an observation and modelling study

Agnese Petteni[1,2], Mathieu Casado[2], Christophe Leroy-Dos Santos[2], Amaelle Landais[2], Niels Dutrievoz[2], Cécile Agosta[2], Pete D. Akers[3,4], Joel Savarino[4], Andrea Spolaor[5], Massimo Frezzotti[6] and Barbara Stenni[1]

[1]Ca' Foscari of Venice, Department of Environmental Sciences, Informatics and Statistics, Mestre (Venice), Italy
[2]LSCE/IPSL, CEA-CNRS-UVSQ, Université Paris-Saclay, Gif-sur-Yvette, France
[3]Geography, School of Natural Sciences, Trinity College Dublin, Ireland
[4]Université Grenoble Alpes, CNRS, IRD, Grenoble INP, INRAE, IGE, F-38000 Grenoble, France
[5]Institute of Polar Sciences, National Research Council of Italy, Venice, Italy
[6]Roma Tre University, Department of Science, Rome, Italy

Correspondence to: Agnese Petteni (agnese.petteni@unive.it)

Abstract.

Water stable isotopes ($\delta^{18}O$ and δD) from ice cores are ~~commonly~~ widely used to reconstruct past temperature variations ~~because~~ through~~of~~ their well-established relationship with local air temperature, commonly referred to as "*isotopic paleothermometer*". However, depositional and post-depositional effects lead to large uncertainties ~~to~~ in the use this proxy in Antarctica. ~~.~~ The magnitude of these uncertainties strongly depends on site location, with larger impacts in low-accumulation regions of East Antarctic Plateau. Depositional effects ~~are largely influenced by the~~include origin of ~~precipitation~~ moisture, which exhibits asymmetries shaped by the continent's geographical and topographical features~~. Additionally~~, as well as precipitation intermittency, which ~~- especially in low-accumulation areas -~~ introduces aliasing in the ~~recorded~~ archived signal~~, limiting the temperature signal that can be retrieved~~. Post-depositional processes, such as sublimation and firn-atmosphere exchange, ~~can~~ further alter the isotopic composition of snow before its transformation into ice, ~~potentially modifying~~thereby modifying the correlation between $\delta^{18}O$ and ~~air~~ temperature ~~for snow samples~~. Here, we present new water isotope measurements from surface snow collected during the East Antarctic International Ice Sheet Traverse (EAIIST), across a remote region of the East Antarctic Pplateau. The traverse - crossing a transitional zone between predominately Indian and Pacific moisture sources - provides ~~direct~~ unique insights into the key role of air mass origin in shaping the isotopic composition of snow ~~$\delta^{18}O$-temperature relationship~~. Comparison with LMDZ6iso simulations indicates that the model successfully captures the spatial variability of $\delta^{18}O$-temperature relationship between different basins, with statistically significant correlations ($p < 0.05$) when the analysis is extended to the Antarctic dataset. This ~~result~~ agreement ~~also~~ further suggests the model's ability to predict the temporal slope required ~~to~~ for calibratinge isotopic ice~~-~~-core records ~~for~~ used for ~~past~~ temperature reconstructions, even in regions ~~where precipitation events originate from~~influenced by multiple ~~different~~ moisture sources. Temporal slopes based on monthly precipitation values range from 0.4 to 0.5 ‰ $°C^{-1}$ for the EAIIST drilling

sites. Finally, we quantify the impact of sublimation on isotopic composition of surface snow δ^{18}O and *d-excess* (an effect that must be considered for accurate paleoclimatic reconstructions.) is evidenced for the region covered by EAIIST. Including sublimation in the modelling of surface snow reduces the discrepancy between observed and modelled values, compared to simulations accounting precipitation, from 1.9 to 1.3 ‰ for δ^{18}O and from 6.6 to 2.9 ‰ for *d-excess*. These results highlighting the key role of this post-depositional process on the Antarctic Plateau. modulization of surface snow

1. Introduction

Ice cores are valuable archives of past climatic and environmental conditions through many environmental proxies both trapped in the ice, such as air bubbles and aerosols, as well as the ice itself, such as its stable water isotopic composition. In East Antarctica, water stable isotopes (δ^{18}O and δD) from the deepest ice cores have been used to reconstruct past temperatures extending back 800,000 years (EPICA community members et al., 2004; Jouzel, 2007), and recent efforts aim to extend these reconstructions to 1.5 million years (Beyond EPICA Oldest Ice Core - Parrenin et al., 2017; Lilien et al., 2021). In this region, ice core temporal resolution is typically limited to multi-annual to multi-decadal scale (Ekaykin et al., 2002; Baroni et al., 2011; Münch et al., 2016). This limitation is due to low accumulation rates and intermittency of precipitation which cause aliasing of the climatic signal recorded by sporadic snowfall events (Ekaykin et al., 2016; Laepple et al., 2018; Casado et al., 2020; Münch et al., 2021). However, ice cores in high-accumulation coastal regions of Antarctica cover shorter temporal ranges but provide finer temporal resolution that can capture seasonal-scale variations (Casado et al., 2023).

Several studies have reported the empirical linear relationship between the isotopic composition of snow and local temperature (Dansgaard, W., 1964; Lorius et al., 1969; Lorius and Merlivat, 1977; Touzeau et al., 2016).

Nevertheless, this relationship is not stable in time and space, as widely documented by direct snow observations and model results (Goursaud et al., 2018; Jouzel, 1997). These variations are related to changes in evaporative conditions and transport pathways to condensation sites which influence the isotopic equilibrium and kinetic fractionation processes at each step of the distillation trajectories (Charles et al., 1994; Masson-Delmotte et al., 2011; Werner et al., 2011, Casado et al., 2017). In addition, the second order parameter deuterium excess (*d-excess* = δD – 8* δ^{18}O, Dansgaard, W., 1964) is highly sensitive to kinetic effects occurring both during evaporation at the ocean surface and along distillation pathways during atmospheric transport. As a result, while over the ocean *d-excess* is —very sensitive to near-surface relative humidity and weakly to temperature, it exhibits the opposite behaviour in central East Antarctica, where it may reflect, at least partially, different moisture origins. (Petit et al., 1991; Risi, 2013; Vimeux, 1999; Jouzel, 2003; Masson-Delmotte et al., 2005; Neumann, 2005). HowerAdditionally, the reliability of water isotopes as climate proxy from ice core *d-excess* in tracking air mass trajectories is debated due to the local influence of post-depositional processes in the snowpack. These processes can alter the snow isotopic composition during prolonged exposure at the atmosphere-snow interface and modify the original precipitation's isotope-temperature relationship (Petit, 1982; Stenni et al. 2016, Touzeau et al., 2016, Casado et al., 2018). Key post-depositional

mechanisms include wind-driven snow redistribution and vapor exchange with the atmosphere, such as sublimation~~., water vapor exchange,~~ condensation processes, ~~wind-driven snow redistribution,~~ snowmelt and vapor diffusion within the snowpack driven by forced ventilation (Steen-Larsen et al., 2014; Beria et al., 2018; Casado et al., 2018; Wahl et al., 2022; Ollivier, 2025). Among these, sublimation plays an ~~particularly~~ important role especially during the warmer months, ~~as it can significantly~~decreasing ~~lower~~ d-*excess* values (Landais et al, 2017, Casado et al, 2021).

These post-depositional alterations are poorly understood and often overlooked in climatic reconstructions, underscoring the need to better constrain the processes shaping the isotope-temperature relationship in surface snow to improve the reliability of ice core-based temperature estimates (Xiao et al., 2013; Ma et al., 2020).

In this study, we investigate the isotopic composition of ~~surface~~ snow ~~snow~~ samples collected roughly every 20 km during the East Antarctic International Ice Sheet Traverse (EAIIST - Traversa et al., 2023) in 2019-2020. The dataset includes both surface snow and bulk samples, which reflect precipitation over time scales ranging from seasonal to multi-annual periods, respectively. This scientific traverse extended from the coast in Adélie Land into the high interior of the East Antarctic Plateau. ~~Along this route, we identify a marked transitional zone in moisture origin between the Indian and Pacific Oceans that fell over the past decade.~~ We assess the influence of ~~these~~ Indian vs Pacific Ocean ~~distinct~~moisture sources on the spatial variability of the relationship between $\delta^{18}O$ composition of snow and the 2 m air temperature. In addition, we present the *d-excess* vs $\delta^{18}O$ relationship, ~~showing~~ which reveals ~~different~~the ~~different~~ supersaturation pathways ~~observed in~~under cold conditions. To place our results in a broader context, we compare them with a subset ~~provide a broader context, we extend our analysis to~~ of surface snow samples from Indian and Pacific sectors of ~~the previous~~ Antarctica, drawn from the ~~snow~~ dataset compiled by Masson-Delmotte et al.~~,~~ (2008).

~~We then evaluate the ability of the A comparison between observations and simulated water stable isotopes of snow precipitation, through the~~ atmospheric general circulation model LMDZ6iso ~~confirms~~ to reproduce the ~~model's~~ observed ~~ability to correctly predict the~~ $\delta^{18}O$-temperature spatial ~~spatial~~ slope by comparing surface snow observations with modelled precipitation.~~s~~ ~~.~~Subsequent to the spatial analysis, we further assess the model's capability to reproduce temporal slopes, which are commonly used in paleoclimate reconstructions of temperature from ice cores.

~~Subsequently, the model's use in further defining temporal slopes based on the variation of moisture origins – crucial for paleoclimatic reconstructions from ice cores – is investigated as well.~~ Finally, surface snow samples collected along the plateau during the outward and return ~~ways~~paths of the traverse provide an opportunity to assess post-depositional isotopic modification over time. By comparing the observations with precipitation model outputs, we ~~can~~ isolate the impact of ~~post-depositional~~sublimation effect~~s~~ on the snow during summer months. This quantification is achieved by applying a metamorphism model proposed by Casado et al. (2021).

2. Methods

2.1. Geographical area EAIIST

The EAIIST traverse took place during the austral summer 2019-2020. The traverse started in coastal Adélie Land, near the high accumulation site of Dumont D'Urville (DDU: 66°39' S, 140°01' E; elevation = 47 m a.s.l.; mean annual temperature of -10.8°C), until the interior plateau site of Megadune (MD: 80°35' S, 121°35' E; elevation = 2973 m a.s.l), and then returned along the same route back to DDU (Fig. 1a). The traverse route passed by the Dome C site (DC: 75°06' S, 123°23' E; elevation = 3233 m a.s.l.; mean annual temperature of -54.5°C) where the EPICA ice core was drilled (EPICA community members et al., 2004) and where the Concordia station is currently located. Dome C represents the maximum elevation of the traverse. ~~Although the traverse is topographically divided at Dome C, the transition between the predominance of Indian and Pacific air mass origins occurs farther south (see Results).~~

2.2. EAIIST snow samples and isotope measurements

Two types of surface snow samples were collected: 85 surface samples, representing the upper 3 cm of snow, and 52 bulk samples, consisting of snow integrated over a vertically dug 1 m-deep snowpit. Surface samples were taken at each stop during daytime approximately every 20 km along the 1,600 km route from DDU to MD, and onward to DC. A single surface sample at one location was obtained by mixing snow from 10 locations randomly selected over a similar area of 100 x 100 m, representing an average. Bulk sampling required longer processing time digging 1 m deep snowpit and scratching the snow along the vertical profile and was therefore carried out only during lunch and evening stops. ~~Snow samples were collected approximately every 20 km over 1,600 km route. Furthermore, the traverse included the collection of additional surface snow samples during the return journey MD to Dome C. Two types of surface snow samples were collected: 85 surface samples (top 3 cm of snow) and 52 bulk samples corresponding to snow integrated from a vertically dug 1 m deep snowpit.~~ The samples were collected with 50 mL Corning tubes which were sealed to prevent air exchange and kept frozen until arrival to laboratories in Europe. ~~The s~~Samples were distributed between the *Laboratoire des Sciences du Climat et de l'Environnement* of Paris (LSCE, France) and *Ca' Foscari University* of Venice (UNIVE, Italy) for water isotopic analysis. The samples were melted only immediately prior ~~to~~ the measurement to minimise potential alterations of the water isotopic composition. Analyses were performed using a Cavity-Ring Down Spectroscopy (CRDS) analyser PICARRO model L2130-i at UNIVE and LSCE.

The isotopic composition of snow is expressed in delta-notation (‰) (Craig, 1961) relative to laboratory standards, which were previous calibrated against the international standards V-SMOW (Vienna Standard Mean Ocean Water) and V-SLAP (Vienna Standard Light Antarctic Precipitation). The accuracy of PICARRO measurements was determined as the mean difference between measured and true values of laboratory standards, with uncertainty represented by their standard deviation. This yielding an accuracy of -0.01 ‰ for $\delta^{18}O$, -0.07 ‰ for δD, and -0.02 ‰ for *d-excess*, with corresponding uncertainties of ±0.07 ‰, ±0.4 ‰, and ±0.4 ‰. Previous inter-calibration experiments revealed mean discrepancy between UNIVE and LSCE measurements of the same samples equal to 0.14 ‰ and 0.80 ‰, for $\delta^{18}O$ and *d-excess* respectively (Petteni et al., 2025).

ha formattato: Tipo di carattere: Corsivo

ha formattato: Tipo di carattere: Corsivo

ha formattato: Tipo di carattere: Corsivo

To estimate the order of magnitude of spatial isotopic variability in surface snow at one location, we report the standard deviation (SD) from previous Antarctic datasets. At Dome C (Casado et al., 2018), the local variability is around 3.4 ‰ for $\delta^{18}O$ and 4.1 ‰ for *d-excess* (defined as 2 SD of replicates obtained in an area of 100 x 100 m). ~~During the EAIIST traverse, surface samples were obtained by mixing snow from 10 locations randomly selected over a similar area of 100 x 100 m, representing an average. Therefore~~Since the surface samples correspond at mixed snow from 10 locations, the impact of spatial variability on the error of the mean is expressed as the standard deviation of the mean (also known as standard error, SE):

1) $$SE = \frac{s}{\sqrt{n}}$$

where s is the SD calculated from individual samples and n is the number of subsamples. Applying this, the expected spatial variability for our composite surface samples is 3.4 ‰ / √(10) ~1.1 ‰ for $\delta^{18}O$ and 4.1 ‰ / √(10) ~1.3 ‰ for *d-excess*. Similar SE are observed in the coastal area of Dumont D'Urville, based on the top 2.5 cm of snowpit samples reported by Landais et al., (2017). Overall, while these values can vary across sites separated by hundreds of kilometres, we set an indicative uncertainty arising from local spatial variability of 1.1 ‰ for $\delta^{18}O$ and 1.3 ‰ for *d-excess*, as reference for interpreting our data.

2.3. Antarctic dataset

To provide a broader spatial analysis, we compare our data with the Antarctic surface snow database of Masson-Delmotte et al., (2008), which offers a comprehensive overview of isotopic variability across the continent. From the original dataset, which includes different types of snow samples, we selected surface snow, bulk snow, snowpit and firn cores that capture signal ranging from annual to approximately 20 years, based on sample depth and local ~~accumulation~~ precipitation rates. For the comparison with our snow samples, we divide the dataset in Pacific and Indian sectors, based on Sodemann and Stohl, (2009). To do this, we classified the region at west of 60°W and the area near the Ross Sea as Pacific sector, while the sampling sites located north then 80°S and between 60°E and 180°E as Indian sector.

2.~~4~~3. FLEXPART back-trajectories

The Lagragian particle dispersion model FLEXPART (FLEXible PARTicle) is employed to calculate 10-day back-trajectories of air masses at 12-hour temporal resolution for each sampling site of the traverse located on the Antarctic Plateau. These trajectories are derived for the 500-hPa pressure level, representing mid-tropospheric transport pathways reaching the plateau. With two trajectories calculated per day over the 2009–2019 period, we computed approximately 7,300 trajectories for each site. To allow for a comprehensive multi-annual evaluation and emphasise the air masses leading precipitation events at the

sampling sites, the trajectories were averaged and weighted by ERA5 precipitation rates (see Section 2.54). The classification of air mass origins into Indian, Pacific and Atlantic sectors is based on their latitudinal and longitudinal distributions, as illustrated in Section 3.1, Fig. 2.

2.54. ERA5 climatic signal

We use ERA5 reanalysis data (provided by the European Centre for Medium-Range Weather Forecasts) to estimate the precipitation interval and associated temperature conditions related to snow ~~accumulation~~ precipitation of surface and bulk snow samples (Fig. 1b). ERA5 provides hourly precipitation and temperature values at 0.25° spatial resolution.

Prior to the comparison with ERA5, all snow samples were converted to water equivalent using density values of trench measurements at Dome C (Ooms et al. 2025). The densities are equal to 290 kg m^{-3} for the upper 3 cm of snow and 320 kg m^{-3} for the upper 1 m. For each sample, precipitation events in ERA5 were sequentially accumulated until the target water-equivalent thickness of the sample was reached. Due to the strong gradient in precipitation rates from the coast (100–300 mm w.e. yr^{-1}) to the plateau (20–50 mm w.e. yr^{-1}), surface samples near DDU represent from 1 to 3 months of snowfalls, whereas those collected on the plateau correspond to up to ~6 months. Similarly, bulk samples represent approximately 1 year of precipitation in coastal areas and up to 15 years at the highest-elevation sites. ~~direct represent from 1 to 3 months of snowfallsDue to decreasing accumulation rates from the coast (100-300 mm weq yr^{-1}) to inland sites (20-50 mm weq yr^{-1}), the surface samples near DDU represent a couple of months accumulation compared to up to 6 months of accumulation on the plateau. Bulk samples reflect ~1 year near the coast and up to 15 years on the plateau.~~ This estimate considers only snowfall-driven ~~accumulation~~ precipitation - excluding accumulation coming from clear-sky precipitation, such as diamond dust and vapor condensation (Stenni et al., 2016) or effects from wind redistribution, erosion, ~~or~~ and sublimation—but provides a distinction between seasonal (surface) and multi-seasonal signals (bulk) signals recorded in the samples.

To investigate the $\delta^{18}O$-temperature ($\delta^{18}O$-T) relationship, we compare two temperature metrics. The first is the average 2 m temperature (T) which mainly captures the spatial climatic variability across the continent. The second is the precipitation-weighted temperature (T_{pw}) which has a more temporal emphasis reflecting the thermal conditions during snowfall events. Indeed, T_{pw} is an average temperature where the values are weighted according to the amount of ~~precipitation~~ snowfalls during each time interval. We calculate T and T_{pw} for each sampling site, based on the ~~accumulation~~ precipitation interval corresponding to surface snow samples (see Section 3.1). Furthermore, we calculate the average multi-annual (1980-2020) temperature for both EAIIST and Antarctic snow isotopic database (Masson-Delmotte et al., 2008), enabling a consistent spatial analysis for samples collected during different campaigns.

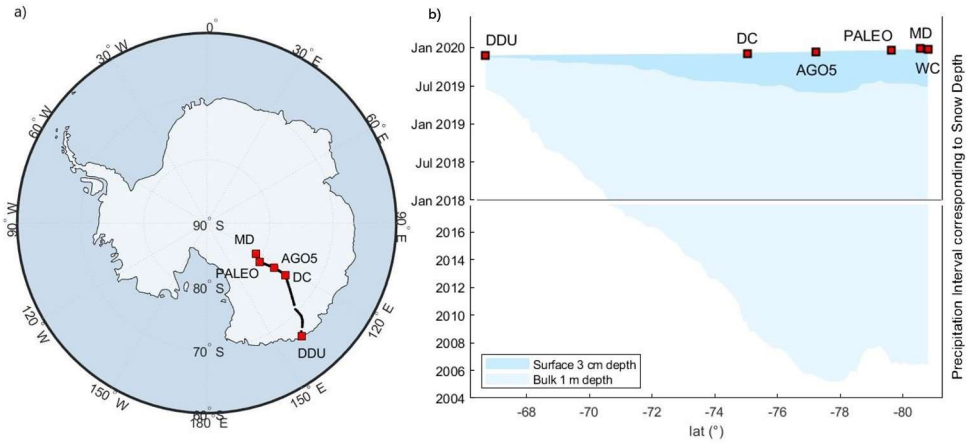

Figure 1. a(left) Map of EAIIST traverse and with principal sampling sites. b(right) precipitation Accumulation period derived from (from ERA5,) corresponding to surface and bulk snow samples across the traverse. Main sampling sites are marked with red squares: Dumont D'Urville (DDU), Dome C (DC), AGO5, PALEO, and Megadune (MD).

2.65. LMDZ6iso model data

LMDZ6iso (Risi et al., 2010) is the isotope-enabled version of the atmospheric general circulation model (AGCM) LMDZ6 (Hourdin et al., 2020). We use the LMDZ6iso version 20231022.trunk with the NPv6.3 physical package (Hourdin et al., 2023), which is nearly identical to the IPSL-CM6A atmospheric setup (Boucher et al., 2020), used for phase 6 of the Coupled Model Intercomparison Project CMIP6 (Eyring et al., 2016). We use LMDZ6's standard horizontal Low Resolution (LR) longitude-latitude grid (144×142), which corresponds to a 2.0° resolution in longitude and 1.67 ° in latitude. The vertical grid comprises 79 levels, with the lowest atmospheric level approximately 7 m above ground level (AGL) at Dome C. The simulation is nudged towards 6-hourly three-dimensional fields of temperature and wind from the ERA5 reanalysis (Hersbach et al., 2020), using a relaxation time scale of 3 hours. Nudging is excluded below the sigma-pressure level equivalent to 850 hPa above sea level, allowing the physics and dynamics of the model to operate freely within the boundary layer. Surface ocean boundary conditions are derived from ERA5 reanalysis monthly mean sea surface temperature and sea-ice concentration fields. The simulation used in this study is described and evaluated over Antarctica in Dutrievoz et al., (2025). Snow samples are simulated by stacking precipitation events until reaching the target thickness, corresponding to surface and bulk sample depths. The snow layers are precipitation-weighted before averaging, ensuring consistency when compared with the surface

and bulk snow data. The error in LMDZ6iso precipitation at Concordia, defined as the difference between modelled and observed values for a supersaturation parameter $\lambda = 0.004$ K_s^{-1}, is 4.0 ‰ for $\delta^{18}O$ and 1.9 ‰ for *d-excess*.

ha formattato: Apice

ha formattato: Tipo di carattere: Corsivo

2.76. Snow metamorphism model

The snow metamorphism model proposed by Casado et al., (2021) describes the relative isotopic variations in snow induced by different processes. Additionally, the model quantifies the flux of water transferred from the snow to the atmosphere, starting from the isotopic composition of surface snow remaining after sublimation $R_{sub\text{-}snow}$, as described the following Eq. 2:

$$R^i_{sub\ snow} = \alpha^i_{eq-su}\ (T)\text{-}\left[R^i_{snow}\left(\frac{D^i}{D}\right)^k(1 - RH) + RH \cdot R^i_a\right] \quad 2)$$

Where R_{snow} is the initial composition of the snow, D^i and D are the keinetic diffusivity coeffients, $\alpha_{eq\text{-}sub}$ is the fractionation coefficient related to sublimation, RH is the relative humidity (Merlivat and Jouzel, 1979) and R_a is the isotopic composition of atmospheric vapor. The exponent k is the roughness parameter (Craig and Gordon, 1965) , here set to 0.4. In particular, the model predicts that sublimation during the warmest months lead to a *d-excess* / $\delta^{18}O$ slope steeper than -2 ‰ / ‰, whereas precipitation input follows a slope of -0.5 ‰ / ‰.

The isotopic difference between R_{snow} and $R_{sub\ snow}$ (expressed as ratio) is used to compute the flux of water transfered from the snow to the atmosphere. This computation takes into account the fractionation coefficient associated to sublimation and the initial water quantity of the snow sample. This approach will be used in Ssection 4.23.6, to isolate the impact of sublimation in surface snow, comparing the outbournd and return samples of the traverse.

In addition, we simulate the final composition of the snow, starting from the outbound ~~outboud~~ values and incorporating the snow precipitation input from LMDZ6iso model and taking into account the contribution of sublimation effects for the number of ~~free~~ precipitation-free days.

3. Results

3.1. Air mass back-trajectories

We present precipitation-weighted air mass back-trajectories over the decadal period 2009-2019 for four representative plateau sites (Fig. 2). At Dome C, 9590% of the back-trajectories originates from the Indian Ocean (red), as expected for this part of the East Antarctic Plateau (Sodemann and Stohl, 2009). Although the traverse is topographically divided at Dome C, the transition between the predominance of Indian and Pacific air mass origins occurs farther south. At AGO5, approximately 70 % of precipitation events are associated with the Indian sector, with a secondary influence from Pacific Ocean (blue). Southern sites like PALEO and MD, are influenced by the Pacific Ocean, which accounts for over 85 % of precipitation events, with minor contributions from the Indian (5%) and Atlantic (10%) sectors. Based on these observations and the findings of Sodemann and Stohl, (2009) we set the transition between predominately Indian-sourced to predominately Pacific-sourced air

masses at approximately 78°S along the EAIIST route (see Appendix A, Fig. A1). Note that these air-mass origins are more representative of the bulk samples rather than the surface snow, as they are computed as the average over ten years.

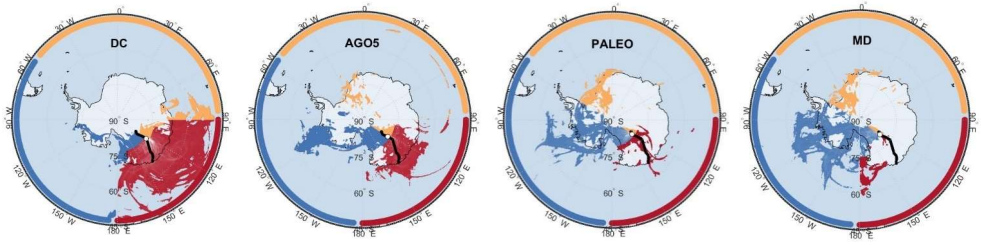

Figure 2. Precipitation-weighted air mass back-trajectory distributions for the period 2009–2019 at four key sites: DC, AGO5, PALEO, and MD. Colors indicate air mass origins: ~~, with red, blue and orange representing the~~ Indian (red), ~~the~~ Pacific (blue) and ~~the~~ Atlantic (orange) ~~o~~Oceans~~, sector, respectively.~~

3.2. ERA5 temperature signal

The $\delta^{18}O$ of surface samples (top 3 cm) collected during the outbound and return ways of the traverse, which represent ~~a time interval of few~~ 5-6 months of snowfalls, exhibits strong ~~correlation~~correlation with both T and T_{pw} (R^2=0.94). However, the two relationships yield different slopes of 0.9 ‰ °C^{-1} and 0.6 ‰ °C^{-1}, respectively (Fig. 3).

The $\delta^{18}O$-T slope is consistent with the value obtained from surface, bulk and shallow snow samples of the Antarctic database (Masson-Delmotte et al., 2008) for Adélie Land based on multi-annual temperature (1980-2020). This similarity validates the use of multi-annual temperature (referred as T in the next Sections) for spatial analysis of snow samples that represent at least an annual signal. On the other hand, the $\delta^{18}O$-T_{pw} slope is very close to that observed for precipitation at Dome C (0.5 ‰ °C^{-1} - Dreossi et al., (2024)), suggesting that the $\delta^{18}O$-T_{pw} relationship is closer to approximating the temporal relationship between snow isotopes and local weather.

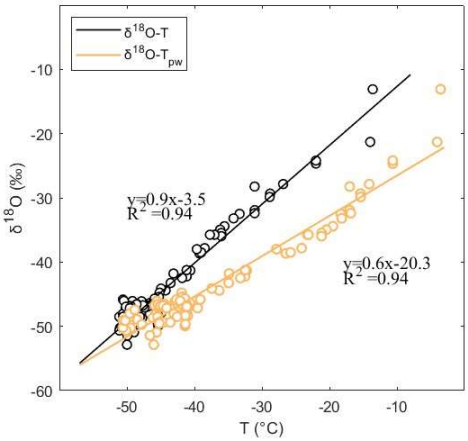

Figure 3. δ^{18}O-T vs δ^{18}O-T_{pw} relationships evaluated for surface snow samples, calculating mean temperature and precipitation-weighted temperature over time intervals corresponding to 3 cm of snow ~~accumulation~~precipitation.

3.3. Spatial distribution of bulk isotopic composition

The snow isotopic composition of bulk samples ranges from -20.0 ‰ at the coastal site near DDU to -52.5 ‰ at the most inland Megadune site (a comparison with surface samples is provided in Appendix B, Fig. B1). This range greatly exceeds the uncertainty expected from spatial variability per site (~1.1 ‰, see ~~Methods~~ Section 2.2), and these values fall well within the range of previous Antarctic surface snow isotopic composition (Fig. 4). Between DDU and Dome C, temperature and δ^{18}O both decline in parallel as the altitude increases. ~~However~~Yet, south of Dome C toward Megadune, the temperature increases as the altitude decreases, but δ^{18}O slightly decreases. Similarly, the *d-excess* increases linearly from DDU to Dome C but then remains constant further south. Following our back-trajectory air mass results, we divide the EAIIST snow isotopic dataset into two sections split at 78°S.

Section I~~1~~ (north of 78°S) exhibits the expected linear relationship between isotopic composition of snow and local climatic and geographic parameters (Tab. 1, Fig. 5). These factors include distance from the nearest coast, latitude, elevation and mean annual 2 m air temperature. In contrast, in Section II~~2~~ (south of 78°S), these linear correlations disappear for all the mentioned parameters.

Within Section II~~2~~, where no abrupt temperature variations are observed, two anomalous sites are notable: one located 20 km south of PALEO site, with a δ^{18}O value of -47.9‰, and another at the Windcrust site (WC) with a value of -48.9‰, roughly 4 ‰ higher than those of the nearby samples. Both sites are also characterised by extremely low *d-excess* values of 7.0‰ and 3.3‰, respectively, compared to those observed on the plateau. Such values likely indicate local sublimation

(Casado et al., 2021; Wahl et al., 2022). Supporting this interpretation, field observations indicate the presence of large hoar crystals at these sites which experience relatively large strong wind, potentially of katabatic origin (Bintanja et al., 1998). Although weaker on the plateau than along the continental margins, these winds can persists for extended periods, creating dry conditions that promote sublimation during summer (Grazioli et al., 2017). In Section ~~3.6 and 4.2~~3.6, we further investigate the impact of sublimation on surface snow based on the comparison between the samples collected during the outward and return ~~legs~~ paths of the traverse.

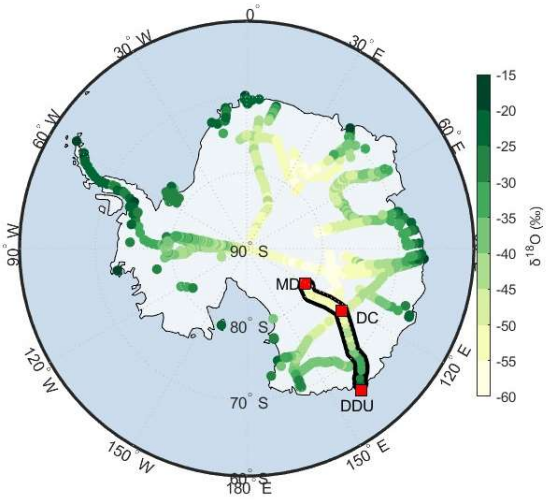

Figure 4. Map of Antarctica showing the distribution of the $\delta^{18}O$ values of EAIIST bulk samples for Section I~~1~~ (from DDU to DC) and Section II2 (from DC to MD), outlined with black contours. Values are shown alongside ~~marked in black countour. The values are reported along with~~ surface, bulk and shallow snow samples from the Antarctic dataset (Masson-Delmotte et al., 2008).

Table 1. Slope and correlation coefficients (R^2) of linear relationships between isotopic composition and geographical/climatic variables, calculated for the Antarctic dataset and Sections I~~1~~ and II2 of the EAIIST traverse. ~~Relationship~~ Relationships are ~~with $R^2 > 0.5$ are~~ shown in bold when statistically significant (defined by $p < 0.05$).

	Distance from coast	Sin of latitude	Elevation	Temperature

		Slope ‰ (100 km)$^{-1}$	R^2	Slope ‰ (°)$^{-1}$	R^2	Slope ‰ (100 m)$^{-1}$	R^2	Slope ‰ °C^{-1}	R^2
Antarctic database	**$\delta^{18}O$**	**-2.1**	**0.71**	0.57	0.00	**-1.0**	**0.76**	**0.9**	**0.90**
	dxs	**0.9**	**0.61**	-0.83	0.01	(above 2000 m) **0.4**	**0.50**	(below -45°) **-0.35**	**0.52**
EAIIST Section I~~1~~ (north 78°S)	**$\delta^{18}O$**	**-2.5**	**0.92**	**496.7**	**0.95**	**-1.3**	**0.80**	**0.98**	**0.95**
	dxs	**0.8**	**0.75**	**-165.21**	**0.75**	(above 2000 m) **0.9**	**0.57**	(below -45°) **-0.62**	**0.54**
EAIIST Section II~~2~~ (south 78°S)	**$\delta^{18}O$**	-0.04	0.00	12.0	0.00	0.36	0.00	-0.16	0.00
	dxs	0.26	0.03	-74.5	0.03	-0.47	0.03	0.10	0.00

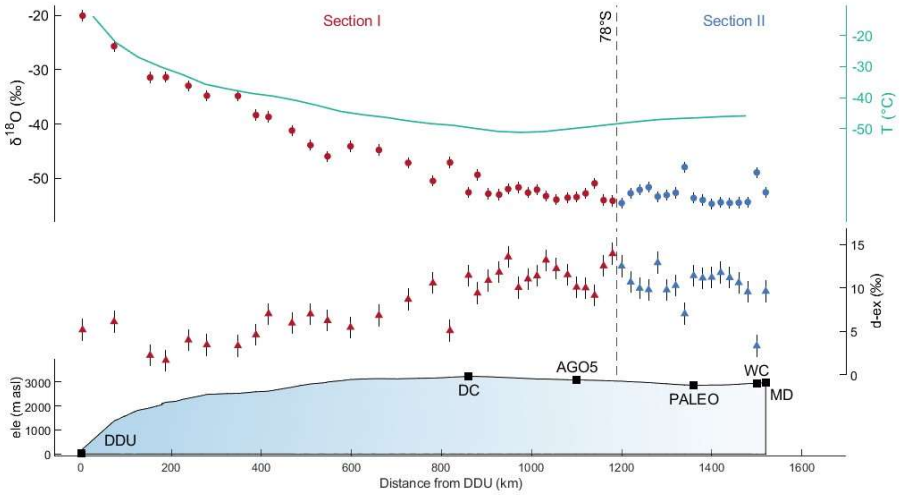

Figure 5. Spatial distribution of $\delta^{18}O$ and *d-excess* values of bulk samples for Section I~~1~~ (red dots – north of 78°S) and Section II~~2~~ (blue dots – south of 78°S). The vertical bars represent the uncertainty associated with local variability. Temperature, elevation and distance from DDU are reported.

3.4. ~~Impact of the~~ Moisture origins impact on isotopic composition: observations vs model outputs

We present the EAIIST and Antarctic datasets subdivided ~~extend the division between~~into Pacific and Indian sectors ~~to the Antarctic database, based on Sodemann and Stohl, (2009). To do this, we classified the region at west of 60°W and the area near the Ross Sea as Pacific sector, while the sampling sites located north then 80°S and between 60°E and 180°E as Indian sector.~~ For the Antarctic dataset, the linear regressions for the $\delta^{18}O$-T relationship independently calculated for each of the two datasets share a common slope of 0.9 ‰ °C^{-1} but differ in intercept by 7.2 ‰ (Fig. 6a ~~– left~~). In the *d-excess* vs $\delta^{18}O$ relationship, under cold condition (i.e. for $\delta^{18}O$ values lower than -45 ‰), the two sectors exhibit distinct compositions, with mean slightly

higher *d-excess* values (~2 ‰) observed for the Indian samples. Instead, in warmer coastal regions, *d-excess* shows higher variability (Fig. 6 b ~~right~~).

The comparison with bulk samples of EAIIST reveals that Section I~~1~~ - primarily influenced by Indian sector – exhibits isotopic values consistent with those of the corresponding divide of the Antarctic dataset. In contrast, Section II2 shows a pattern more aligned with Pacific sector. ~~These aspects will be discussed further in Section 4.1.~~

We compare the observed and LMDZ6iso simulated bulk samples. For $\delta^{18}O$ (Fig. 7a), the mean and standard deviation of the differences between observed and modelled $\delta^{18}O$ values are -0.95 ± 2.24 ‰ (RMSE = 2.41 ‰), following well the different $\delta^{18}O$-T relationships between Indian and Pacific sector as observed in the Antarctic dataset (Appendix C, Fig. C1). For *d-excess* (Fig. 7b), the model overestimates the values for both sectors by approximately 5.5 ± 2.48 ‰ (RMSE = 6.07 ‰).

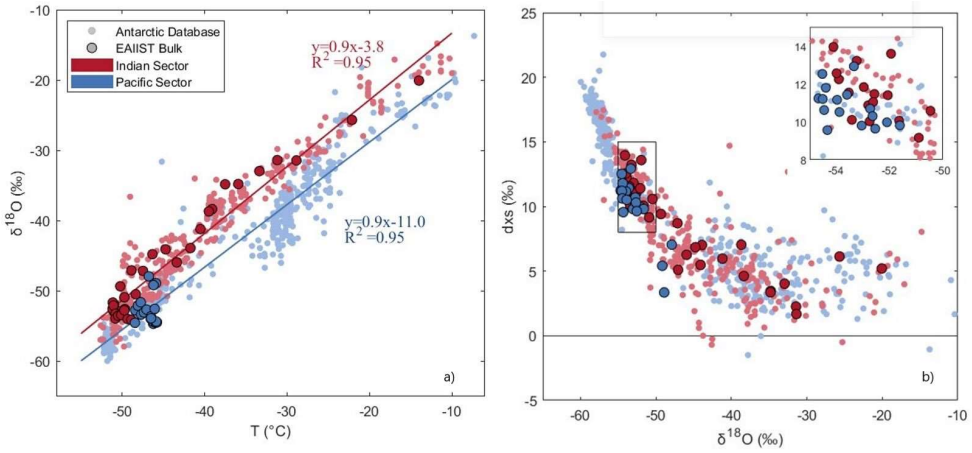

Figure 6. a~~(left)~~ $\delta^{18}O$-T relationship and b~~(right)~~ *d-excess* vs $\delta^{18}O$ for bulk samples of the traverse compared ~~to~~ with Antarctic database for Pacific and Indian sectors.

~~**3.5. LMDZ6iso Data Model**~~

~~Here, we compare modeled $\delta^{18}O$ and d *excess* values for bulk samples simulated by LMDZ6iso with observation (Fig. 7). For $\delta^{18}O$ (Fig. 7 - left), the model successfully predicts the isotopic values, following the different $\delta^{18}O$-T relationship between Indian and Pacific sector as observed in the snow (Appendix C, Fig. C1). For *d-excess*, the model overestimates the values for both sectors by approximately 8 ‰ (Fig. 7 - right). This offset may be attributed to two main factors. First, *d-excess* in the~~

~~model is primarly related to the tuning of the supersaturation parameter for isotopes (λ) within the AGCM. The value of λ equalt to 0,004 K^{-1} is selected to achive a optimal compromise to correctly similate both $\delta^{18}O$ and *d-excess* in surface snow (Dutrievoz et al., 2025). Second, post-depositional processes - not accounted by the model - can alter the isotopic composition of snow after deposition. In particular, as mentioned in Section 3.3, sublimation is commonly linked to a reduction in *d-excess* values (Landais et al., 2017; Wahl et al., 2022) that may partially explain the observed difference in the snow. The influence of sublimation, along with the model's performance in reproducing spatial and temporal slopes, will be further discussed in Section 4.~~

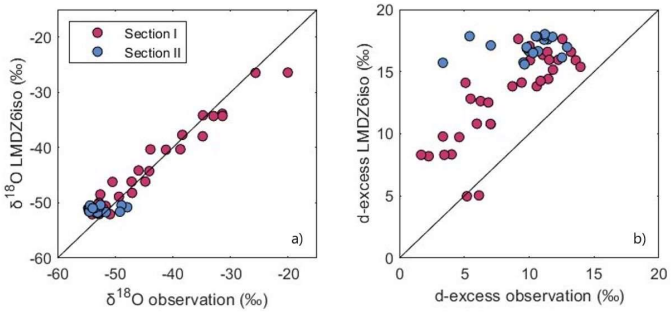

Figure 7. ~~LMDZ6iso vs bulk observations for a(left)~~ $\delta^{18}O$ and b~~(right)~~ *d-excess* LMDZ6iso values vs bulk observations. The black line is for linear regression.

3.~~5~~6. Temporal variability of surface isotopic composition

To assess the impact of post-depositional effects on the isotopic composition of the snow, we compare surface samples (representing a seasonal signal) collected during the outward and return ways of the EAIIST traverse across the plateau region (sampled between 10 and 50 days apart). The return isotopic composition is, on average ~~indeed on average~~, slightly higher for $\delta^{18}O$~~,~~ by approximately 3 ‰ (Fig. 8a), ~~and~~ while~~with a~~ *d-excess* is ~~significantly~~ lower, by 5-10 ‰ (Fig. 8b)~~, on average 5 to 10‰~~. Limited snowfall for most of the sites over the plateau suggests that post-depositional processes could be responsible for the difference observed, allowing for prolonged interaction at the snow-atmosphere interface.

We evaluate the contribution of precipitation to the metamorphism of surface snow between the outward and return journey using the LMDZ6iso simulation outputs. The contribution of precipitation would lead to an increase of up to 2 ‰ for $\delta^{18}O$ and

a decrease of ~1 ‰ for *d-excess* at sites north of 78°S. South of 78°S, the model suggests no change in surface snow isotopic composition due to precipitation. Using ERA5, we investigate the precipitation patterns between the outward and return samplings. In Section I~~1~~, we identify 7-20 precipitation-free days and a total ~~accumulation~~ precipitation of 5-8 mm of fresh snow (corresponding to ~25 % of the surface sample). In contrast, Section ~~2~~II experienced 10-20 dry days with no notable ~~significant~~ precipitation inputs (Fig. 8c).

~~The post-deposition metamorphism leading to isotopic changes in the snow at the surface-atmosphere interface will be discussed in Section 4.2.~~

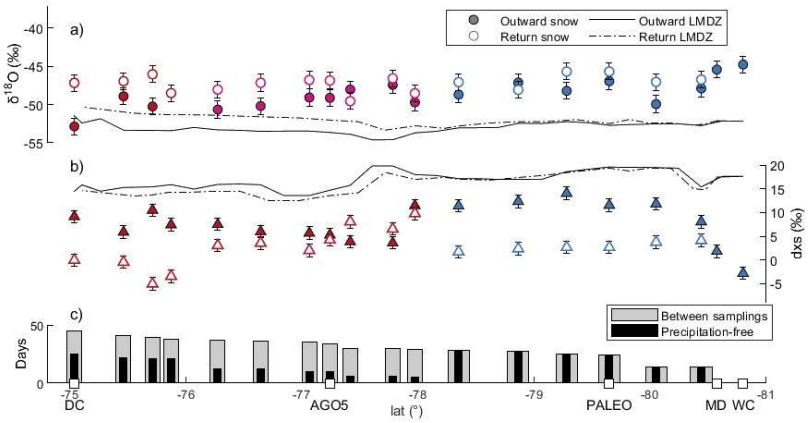

Figure 8. a) $\delta^{18}O$ and b) d-*excess* composition of outward and return surface snow samples (dots) in comparison to the LMDZ6iso model outputs (lines). Vertical bars indicate spatial variability. c) The days between the two journeys (grey) and the precipitation-free days prior the return sampling (black).

3.6. Modelled sublimation effects on surface snow

In Section 3.5, we showed that precipitation input alone could not explain the change of isotopic composition of the surface samples between the outbound and return journeys. Here, we assess whether sublimation - commonly associated with an enrichment in $\delta^{18}O$ along with a decrease of *d-excess* (Dietrich et al., 2023; Hughes et al., 2021) - can explain, at least in part, the variations observed. To this end, we compare the relative variations in *d-excess* and $\delta^{18}O$ against the snow metamorphism conceptual model proposed by Casado et al., (2021), which is able to link the relative change of *d-excess* and $\delta^{18}O$ to the sublimated fluxes in the atmosphere (see Section 2.7). Overall, our observations support this framework: isotopic changes along Section II – during which no precipitation occur according to ERA5 – closely follow the modelled metamorphic modification of isotopic composition characterised by a slope of $dxs / \delta^{18}O$ of -2 ‰ / ‰ (blue dots in Fig. 9) (Casado et al., 2021). For Section I, as shown in Section 3.5, precipitation accounts for a 25% of the return sample weight, as a result, we

expect a mix with the contibution of precipitation, characterised by a slope dxs / $\delta^{18}O$ of -0.5 ‰ / ‰ (Casado et al., 2021). We observe that the surface snow in Section I evolved following a slope of -1.1 ‰ / ‰ (red dots in Fig. 9), which match the hypothesis of an input dominated by sublimation, with a contribution from the precipitation input.

We use Section II data, driven solely by sublimation, to estimate the flux of water transfered from the snow to the atmosphere (eq. Section 2.7). The estimated sublimation fluxes range from 0.04 to 0.09 mm w.e. day^{-1} (Fig. 9), consistent with the range reported in previous studies (0.05–0.35 mm w.e. day^{-1}; Ollivier et al., 2025). It is important to note that the values reported by Ollivier et al. (2025) represent daily estimates and therefore reflect substantial day-to-day variability driven by changes in insolation, cloud cover, temperature, and wind speed. In contrast, our estimates represent averages over periods of up to 50 days. Therefore, they integrate over both days with intense sublimation and days with limited or no sublimation (e.g., cloudy or snowy conditions), resulting in a narrower overall range.

We use this sublimation impact for modeling the final composition of the snow along the whole traverse, using outward snow samples as the initial condition. This calculation accounts for the number of precipitation-free days between samplings (from ERA5), and incorporates precipitation input from the LMDZ6iso model. The final $\delta^{18}O$ and *d-excess* modeled composition is estimated as:

$$\text{Final Snow}_{\text{model}} = \text{Initial Snow}_{\text{obs.}} + \text{Precipitation Input}_{\text{LMDZ6iso}} + (\text{Sublimation x N°}_{\text{dry days}})$$

The difference between observed versus modelled final values are shown in Figure 10. Red symbols represent Section I sampling sites, characterized by high precipitation (> 1 mm w.e.) between outbound and return samplings, for which freshly precipitation represents ~25% of the sampled snow. Blue symbols represent Section II sites with low precipitation (< 1 mm w.e.), characterised by negligible precipitation. The modelled values are presented considering either only the precipitation input or both precipitation and sublimation effects. Including sublimation in the computation reduces the discrepancy for all Section II sites and for the majority of Section I sites. The mean absolute difference decreases from 1.9 to 1.3 ‰ for $\delta^{18}O$ ~~d18O~~, and from 6.6 to 2.9 ‰ for *d-excess*.

~~are compared with both and (). The difference between return observations and modelled final values is 0.04 ± 1.61 ‰ for and -0.48 ± 3.83 ‰ for *d-excess* (mean ± std).~~

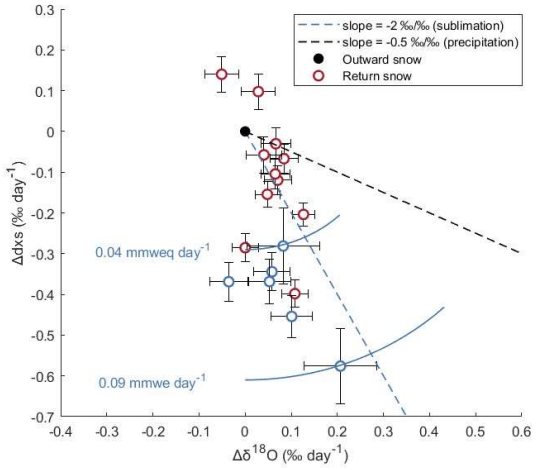

Figure 9. *d-excess* vs $\delta^{18}O$ evolution of snow per day for Section I (empty red dots) and II (empty blue dots) centered on outward composition (black dot), in comparison with modeled dxs/$\delta^{18}O$ sublimation slope (blue dashed line) and precipitation slope (black dashed line). The fluxes relative to sublimation are expressed in mm w.e. day^{-1}. The errorbars represent the uncertainty from spatial variability.

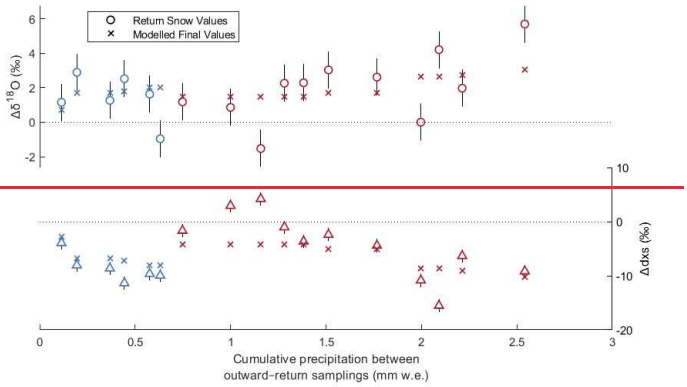

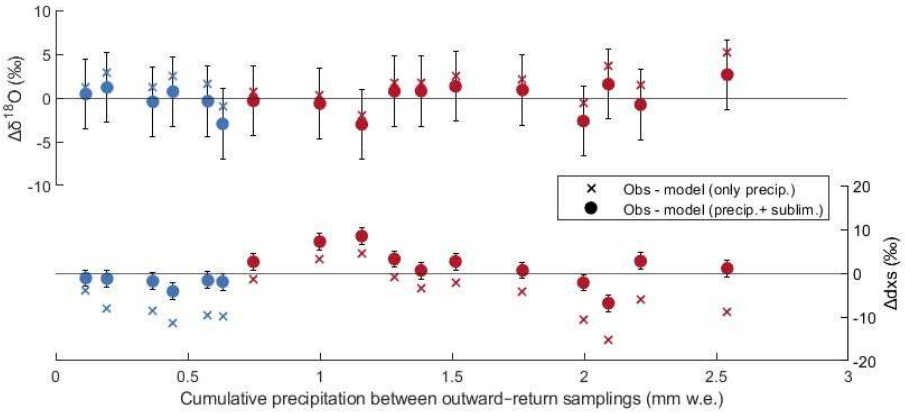

Figure 10. Difference between return-snow observations and modelled $\delta^{18}O$ and *d-excess* values, for Section I (red) and Section II (blue). Modelled values are calculated considering either precipitation only (crosses) or both precipitation and sublimation effects (circles). Error bars represent the uncertainty of the LMDZ6iso model in simulating the isotopic ~~composition~~precipitation at Concordia (Dutrievoz et al., 2025). The x-axis indicates the cumulative precipitation between the outward and return samplings. ~~(empty circles/triangles), (X markers)The x-axis represents cumulative precipitation occurring between outward and return samplings.~~

4. Discussion

4.1. Air mass origins and $\delta^{18}O$-temperature slopes ~~Isotopic Paleothermometer~~

The spatial $\delta^{18}O$-T relationship has traditionally been used to calibrate isotopic paleothermometer (Dansgaard, 1964; Lorius et al., 1969). However, several studies have shown that it is generally less accurate than the $\delta^{18}O$-T temporal slope derived at a single site (Sime et al., 2008; Casado et al., 2017). The EAIIST traverse, which crosses two sectors of East Antarctica influenced by distinct air mass origins yet characterised by relatively similar climatic conditions, provides valuable insights into the role of moisture sources in shaping both spatial and temporal slopes. These observations also highlight the potential to model such relationships in regions where long-term temporal records are not available.

The spatial analysis of EAIIST Section I showed a significant $\delta^{18}O$-T relationship over the Indian sector ($p < 0.05$; Tab. 1), while no significant correlation was detected for Section II. It is important to note that Section II has limited spatial coverage, as the traverse did not extend to the Pacific coast, and the temperature range along this 300 km transect is correspondingly narrow. Therefore, the absence of a detectable correlation cannot be interpreted as evidence that a $\delta^{18}O$–T relationship is lacking in this sector, as confirmed by analysis of the broader Antarctic dataset (Fig. 6a), which shows statistically significant correlations in both sectors ($p < 0.05$). ~~The spatial analysisof revealed (p-value <0.05)over~~The spatial

slopes for the two basins are similar (0.9 ‰ °C^{-1}), ~~- strong correlations with equaltwo distinct δ^{18}O-T relationships for the two sectors investigated (Fig.6 - left). Both relationships are characterised by a slope of 0.9 ‰ °C^{-1},~~ reflecting comparable thermal history of air mass from the coasts to the high-elevation regions in the interior of the continent (Helsen et al., 2007)~~. Yet~~, ~~the~~ while differences in the intercepts are attributed to contrasting vapor isotopic compositions associated with distinct source regions and longer transport pathways for Pacific air masses. ~~differing y-intercept~~

Results from LMDZ6iso model ~~seem to~~ reproduce the inter-sector ~~values suggest contrasting isotopic composition of water vapor, due to different that results to be longer for, likely reflecting both differences in the source ocean regions and in the specific trajectories followed by air masses before reaching the continent.~~

~~As shown in Figure 7a and C1, the inter-sector variation~~ differences in δ^{18}O-T spatial slopes for EAIIST ~~for the spatial slopes~~(Fig. 7a and C1a), and for the broader Antarctic dataset ~~ese findings areed~~(Fig. C2). For this extended dataset, mean δ^{18}O values were calculated over 1980-2000 due to the lack of precise temporal coverage of the snow samples in Masson-Delmotte et al. (2008). Although a comprehensive quantitative evaluation of the LMDZ6iso model is beyond the scope of this study, the qualitative comparison indicates that the model successfully captures the observed spatial variability associated with differing air mass influences. This ,supports the hypothesis that LMDZ6iso is also able to simulate temporal δ^{18}O-T slopese.

Monthly δ^{18}O-T relationships, derived from modelled precipitation at single sites (i.e. Dome C, AGO5, PALEO and MD; Fig. 11), account for varying moisture sources and yield temporal slopes of ~~is reproduced by the model. This result is further supported by Figure C2 (Appendix C), which shows the modelled isotopic values for the Antarctic Dataset, explicitly distinguishing between the two sectors. Because the temporal coverage of the individual samples is not specified by Masson-Delmotte et al., (2008), we adopted a common reference period (1980–2000) and computed mean δ^{18}O values for all samples over this interval.~~

~~These findings suggest that the model has the potential not only to reproduce spatial slopes, but also to predict temporal slopes. To further assess this, we compute monthly precipitation from LMDZ6iso at Dome C, AGO5, PALEO and MD sites accounting for the moisture origin variations (Fig. 9). A temporal δ^{18}O-T slopes between~~ 0.4~~. and~~ 0.5 ‰ °C^{-1} (R^2= 0.89). At Dome C, this prediction is consistent with observed monthly precipitation collected at Concordia Station, which exhibits a temporal slope of ~~temporal slope are retrieved, consistent for the whole spectrum of trajectories.~~ 0.5 ‰ °C^{-1} (Dreossi et al., 2024).

We note that ~~in these lines~~here the term “snow-precipitation samples” refers to both model outputs and precipitation samples collected immediately after deposition where snow was captured on a wooden platform positioned 1 m above the surface to minimize post-depositional alterations. In contrast, the term “snow-surface sample” refers to material collected directly from the surface during the traverse, representing an integrated signal of multiple precipitation events and influenced by wind redistribution and post-depositional metamorphism.~~This slope is similar to the one derived from monthly snow precipitation samples at Concordia Station, Dome C, equal to 0.5 ‰ °C^{-1} (Dreossi et al., 2024).~~

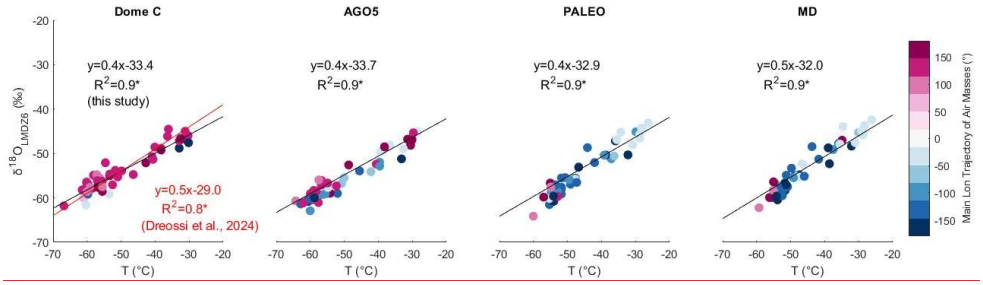

Figure 11. δ^{18}O-T relationship for monthly samples simulated by LMDZ6iso at Dome C, AGO5, PALEO and MD sites. The color scale indicates the dominant longitudinal origin of air masses associated with each monthly precipitation event. Significant linear relationship (p-value < 0.05) is indicated by asterisks.

4.2. Modelled *d-excess* vs δ^{18}O relationship

~~In t~~The *d-excess* vs δ^{18}O ~~comparison~~ relationship (Fig. 6b) shows ~~, the~~ high~~er~~ *d-excess* variability in warmer coastal areas (< 2000 m a.s.l.), reflecting sensitivity to local moisture-source conditions such as temperature, ~~is linked to its preservation of information about changes in close moisture source. These include temperature and~~ relative humidity in evaporative region, ~~as well as fluctuations in~~and sea ice extent. ~~Conversely, in inland regions~~Inland (> 2000 m a.s.l.), at the end of the distillation pathways, *d-excess* becomes more sensitive to condensation temperatures, ~~located at the end of the distillation pathway, the *d-excess* in precipitation becomes more sensitive to condensation temperature,~~ since it is regulated by independent supersaturation functions (Uemura et al., 2012; Stenni et al., 2016; Touzeau et al., 2016; Landais et al., 2017). This ~~behaviour~~ pattern is evident in the~~clearly visible from the~~ Antarctic database and is ~~also~~ weaky detectable in EAIIST for very cold sites ~~slightly evident in the EAIIST data for very cold sites~~ (~~i.e.,~~ δ^{18}O < -50 ‰), ~~with higher *d-excess* values observed for the Indian sector compared to the Pacific sector for the same δ^{18}O composition.~~where Indian-sector samples show slightly higher *d-excess* than Pacific-sector samples at similar δ^{18}O values.

LMDZ6iso model does not accurately predict the *d-excess* values, showing a RMSE equal to 6.07 ‰ (Fig. 7b and C1b). The mismatch primary arises from the model formulation of the isotopic supersaturation parameter (λ) in the AGCM. The chosen value of λ equal to 0.004 K^{-1} is selected to achive a optimal compromise to correctly simulate both δ^{18}O and *d-excess* in surface snow, but leads to a systematic overestimation of *d-excess* (Dutrievoz et al., 2025). In addition, the model do not include post-depositional processes. Sublimation lowers *d-excess* in surface snow by modifying isotopic composition after deposition (Landais et al., 2017; Wahl et al., 2022). This effect is particularly evident in the observations at Windcrust site (WC; Fig. 5), where low *d-excess* values (~4 ‰) reflect strong wind activity, substantial erosion of accumulation, and enhanced snow–

atmosphere exchange. The influence of wind-snow redistribution and sublimation on the isotopic signal is discussed in detail in Section 4.3.

4.3.

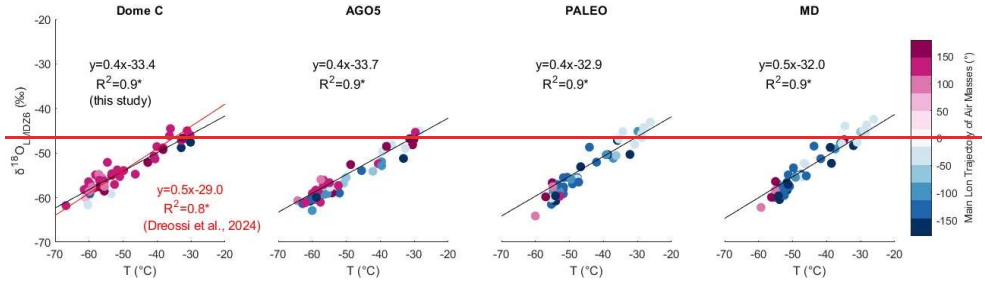

Figure 9. δ^{18}O-T relationship for monthly samples simulated by LMDZ6iso at the sites Dome C, AGO5, PALEO and MD. The color scale indicates the dominant longitudinal origin of air masses associated with each monthly precipitation event. Significant linear relationship (p-value < 0.05) is indicated by asterisks.

Impact of post-depositional processes

On the Antarctic plateau, post-depositional effects mainly include wind-driven snow redistribution, and sublimation. Wind Snow redistribution transport by wind is a relatively "local" process, typically mixing snow from the surrounding areas and one of the main contributions to stratigraphic noise (Hirsch et al., 2023). Studies suggest that the snow shuffled by wind redistribution can reach distances up to ~100 km transporting snow particles over distances of up to ~100 km (Scarchilli et al., 2010; Frezzotti et al., 2007). Such mixing generates stratigraphic effect between precipitation events, leading to Accumulation associated with wind transport is generally limited and occurs primarily in areas such as mega-dune zones, while the main transport mixes the snow particles and occurs over only a few tens of kilometres, corresponding to an elevation difference of 40–60 m. This redistribution generates variability in surface properties between precipitation events, producing stratigraphic noise. For instance, mixing of surface snow has been shown to result in δ^{18}O variability standard deviations of up to 4.4 ‰ within the uppermost 6 cm over a 50 m transect at Kohnen Station in the plateau interior (Münch et al., 2016). In our dataset, such this variability effect is reduced by averagingbecause we mixed surface snow collected over an extended area at each sampling site and by integrating 1 m of snow depth for bulk samples. (see Methods).

To quantify sublimation, mainly impacting the snow metamorphism in summer, we comparedAdditionally, as noted in Section 3.3, sublimation directly modifies the isotopic composition of snow by reducing *d-excess* values . Its effect is particularly observed at the Windcrust site (Fig. 5 - WC), where low *d-excess* values of 4 ‰ reflects the strong wind activity, resulting in substantial erosion of annual accumulation and enhanced sublimation at the snow–atmosphere interface.

Formattato: Nessun elenco puntato o numerato

~~In this study, w~~ surface snow samples collected during the outbound and return ways of the traverse, where low precipitation and strong snow drift favour prolonged summer atmosphere-snow exposure. Assuming 20 precipitation-free days per summer season, we estimated a sublimation-induced variation corresponding to +2 ‰ yr^{-1} in $\delta^{18}O$ and -8 % yr^{-1} in *d-excess* (see Section 3.6).

Including this sublimation effect in the modelled isotopic predictions substantially improved the agreement with observations, reducing the discrepancy for ~~modelledsurface snow observationss exhibitwith 4.94 3.70~~ *d-excess* compared to simulations considering precipitation input alone (Fig. 10).

This improvement is particularly evident at sites where cumulative precipitation between samplings is negligible (< 1 mm w.e.). The remaining differences and variability between observed and modelled values can be partially attributed to uncertainties in ERA5 precipitation and LMDZ6iso model. Previous studies have shown ERA5 overestimates precipitation over the East Antarctic Plateau, with biases reaching up to 50% relative to satellite-based measurements (Roussel et al., 2020). As a result, our modelling likely represents the maximum contribution of precipitation, implying that the metamorphism would be even greater if actual precipitation were lower. We emphasize that the aim of this study is not to quantify the ability of the combined ERA5-LMDZ6iso in reproducing the absolute isotopic values, but rather to evaluate whether accounting sublimation improved the qualitative representation of surface snow isotopic composition compared to precipitation-only scenarios. These results further reinforced the key role of post-depositional processes in shaping the isotopic composition of surface snow.

~~This difference is larger than the one obtained forsamples, likelystrongeringthe effect of is included (Fig. 10)es0.04 ± 1.61 – 0.48 ± 3.81~~

~~part of the methamorphism.~~

~~We acknoweledge that previous studies have shown ERA5 to overestimte precipitation over the East Antarctic Plateau, with biases reaching up to 50% relative to satellite-based measurements (Roussel et al., 2020). As a result, our modelling is based on the maximum contribution of precipiation, implying that the metaamorphism would be even greater if actual precipitation were lower. Overall, this uncertainty further reinforcespost-depositional processesthe isotopic composition of surface snow.The high standard deviations indicate that an additional component of variability – likely associated with stratigraphic noise – remains not represented by our prediction. Nonetheless, the findings confirm that the proposed model reliably reproduces isotopic changes driven by sublimation and underscores the important role of sublimation in shaping the isotopic composition of surface snow in this region.In Section 3.6, we showed that precipitation alone could not explain the change of isotopic composition of the surface samples between the outbound and return journeys. Here, we assess whether sublimation – commonly associated with an enrichment in $\delta^{18}O$ along with a decrease of *d-excess* (Dietrich et al., 2023; Hughes et al., 2021) – can explain, at least in part, the variations observed between the outbound and return surface snow samples. To this end, we compare the relative variations in *d-excess* and $\delta^{18}O$ against the snow metamorphism model proposed by Casado et al., (2021) (see Section 2.6). Overall, our observations support this framework: isotopic changes along Section 2 – during which no precipitation occur according to ERA 5 – closely follow the modelled metamorphic modification of isotopic~~

composition characterised by a slope of dxs / $\delta^{18}O$ of -2 ‰ / ‰ (blue dots in Fig. 10) (Casado et al., 2021). For Section 1, as shown in Section 3.6, precipitation accounts for a 25% of the resurn sample weight, as a result, we expect a mix between the contibution of precipitation, characterised by a slope dxs / $\delta^{18}O$ of -0.5 ‰ / ‰ (Casado et al., 2021). We observe that the surface snow in Section 1 evolved following a slope of -1.1 ‰ / ‰ (red dots in Fig. 10), which match the hypothesis of an input dominated by sublimation, with a contribution from the precipitation input.

We use Section 2 data, driven solely by sublimation, to estimate the flux of water transfered from the snow to the atmosphere (eq. Section 2.6). The resulting sublimation fluxes range from 0.04 to 0.09 mm weq day^{-1} (Fig. 10), consistent with values reported by Ollivier et. al., (2025), who observed sublimation-driven vapor fluxes ranging from 0.05 to 0.35 mm weq day^{-1} during summer at Dome C. We use this isolated sublimation impact for modeling the final composition of the snow along the whole traverse, using outward snow samples as the initial condition. This calculation accounts for the number of precipitation-free days between samplings (from ERA5), and incorporates precipitation input from the LMDZ6iso model. The final $\delta^{18}O$ and d-$excess$ modeled composition is estimated as:

$$\text{Final Snow}_{\text{model}} = \text{Initial Snow}_{\text{obs.}} + \text{Precipitation Input}_{\text{LMDZ6iso}} + (\text{Sublimation x N°}_{\text{dry days}})$$

When accounting for sublimation effects, the predicted isotopic values showed better agreement with the observed variability in the return snow samples (Fig. 11) compared to the simulation from the LMDZ6iso model alone (Fig. 8). These findings highlight the signficant impact of sublimation – even if limited – on the isotopic composition of surface snow in this region.

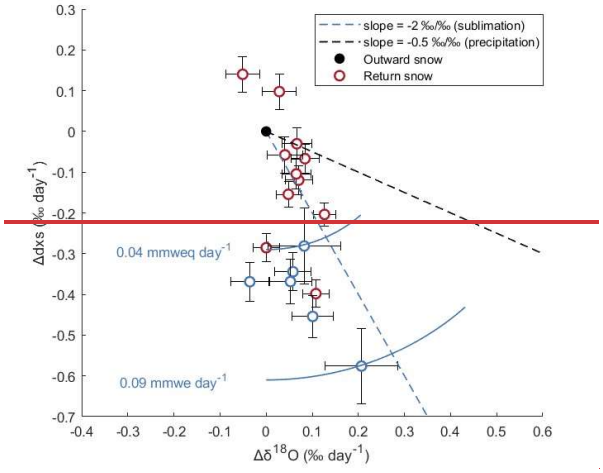

Figure 10. *d-excess* vs $\delta^{18}O$ evolution of snow per day for Sector I (empty red dots) and II (empty blue dots) centered on outward composition (black dot), in comparison with modeled dxs/$\delta^{18}O$ sublimation slope (blue dashed line) and precipitation slope (black dashed line). The fluxes relative to sublimation are expressed in mm weq day^{-1}. The errorbars represent the uncertainty from spatial variability.

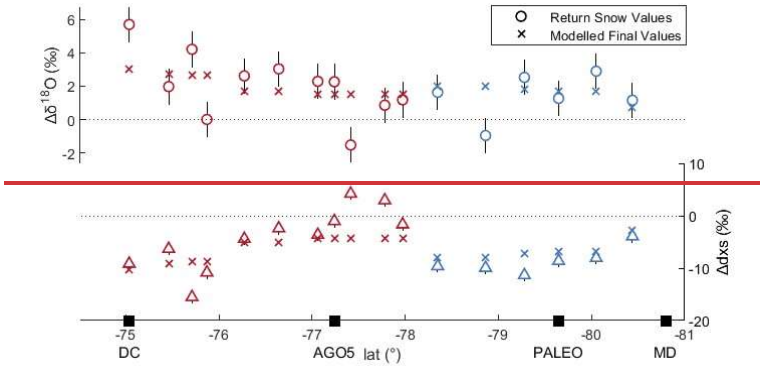

Figure 11. Differences in $\delta^{18}O$ (top) and *d-excess* (bottom) between outward snow samples and (i) return snow values, and (ii) modelled final snow calculated based on both the precipitations input (LMDZ6iso) and the sublimation input. Vertical bars indicate the spatial variability of snow samples.

5. Conclusions

In this study, we presented new observational and modelling evidences on the processes shaping the isotopic composition of surface snow across the East Antarctic Plateau. ~~new isotopic data from surface and bulk snow samples collected along the EAIIST traverse, which covers a remote and previously unexplored region of the East Antarctic Plateau. The traverse crosses a transitional zone between two dominant air mass origins: the Pacific and Indian Oceans. By investigating the δ^{18}O-T and *d-excess* vs δ^{18}O relationships, we identified distinct isotopic signature associated with each sector, highlighting the influence of moisture sources on the snow isotopic composition. These findings were further supported by a spatial comparison with the broader Antarctic snow dataset of Masson-Delmotte et al., (2008).~~

~~The EAIIST dataset also confirmed the ability of the LMDZ6iso model to adequately reproduce the spatial distribution of δ^{18}O in surface snow, accounting for the different moisture origins. Yet, the model showed reduced capability in simulating the *d-excess* values. This limitation can be attributed primarily to model parametrization and secondarily to post-depositional effects, such as sublimation, which significantly affect the *d-excess* signal. The impact of sublimation was assessed by comparing surface snow samples collected during the outbound and return ways of the traverse across the plateau — where low accumulation rate and strong snow drift lead to prolonged summer atmosphere-snow exposure, enhancing this effect. Assuming 20 precipitation-free days per summer season, the associated post-depositional variation could induce an enrichment of +2 ‰ yr^{-1} in δ^{18}O and a decrease of up to -8 ‰ yr^{-1} in *d-excess* (based on an avearge methamorisphism of +0.1 ‰ day^{-1} and -0.4 ‰ day^{-1} during summer, see Section 4.6).~~

~~In conclusions, t~~Together, these~~hese~~ results provide~~d~~ key insights for the future interpretation of ice cores collected ~~along the EAIIST traverse~~in low-accumulation area~~.~~:

~~(~~i) ~~Surface and bulk~~Observational snow samples defined the range of isotopic variability ~~linked~~ associated with~~to~~ distinct moisture ~~-~~source sectors~~s~~, ~~which~~ an essential consideration in ~~must be considered in~~ regions where multiple air ~~-~~mass trajectories coexist and ~~possibly vary~~may shift over time.

~~(~~ii) The comparison between observations and LMDZ6iso outputs confirmed the model's ability to ~~capture~~ reproduce both spatial and temporal δ^{18}O-T slopes. ~~In particular, the~~ The temporal slope, in particular, ~~of 0.5 ‰ °C^{-1} — previously established from precipitations at Dome C (Dreossi et al., 2024) and commonly used to calibrate the isotopic records from this site — is validated for all the sites in the EAIIST transition region. This supports its use for calibrating the δ^{18}O-T~~is crucial for calibrating the *paleothermometer* ~~also~~ in areas lacking ~~direct~~ long-term ~~observations~~ records~~in time~~.

(iii) Sublimation has a great influence on the isotopic signal, particularly decreasing *d-excess* in summer. This demonstrates that achieving a robust qualitative assessment of isotopic variability requires the explicit inclusion of isotopic fractionation during sublimation and condensation processes in General Circulation Models (GCMs).

~~While the observed annual scale variation attributed to sublimation is smaller than the inter-sector δ^{18}O differences (Pacific vs Indian origins), it represents a non-negligible factor for accurate reconstruction of past temperature.~~ (iv) ~~Lastly~~Finally, the

finding that relatively close drilling sites (e.g. Dome C and PALEO, separated by ~~separated by only~~only few hundred kilometres) ~~can~~ may record ~~experience different~~ precipitation ~~pathways~~from distinct moisture pathways suggests a promising ~~, could be used as a~~ strategy to enhance ~~the~~ temperature ~~signal~~ reconstructions~~retrieved,~~ combining ice core records that ~~archive~~ capture common large-scale climate variability through different precipitation events.~~the same climatic signal via distinct precipitation events.~~

Appendix

Appendix A: Londitudinal distribution of air mass orising on the East Antarctic Plateau sampling sites

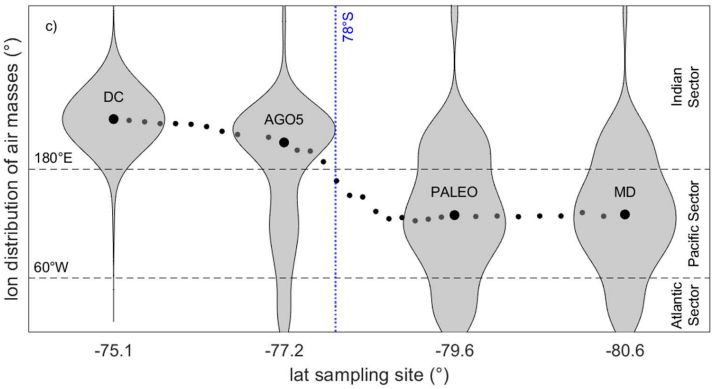

Figure A1. Longitudinal distribution back-trajectories over the 2009–2019 period for four representative sites: Dome C, AGO5, PALEO, and MD. The median longitudinal origin of air masses for the 33 sampling sites across the Antarctic Plateau is indicated by black dots.

Appendix B: Spatial distribution of surface and bulk samples

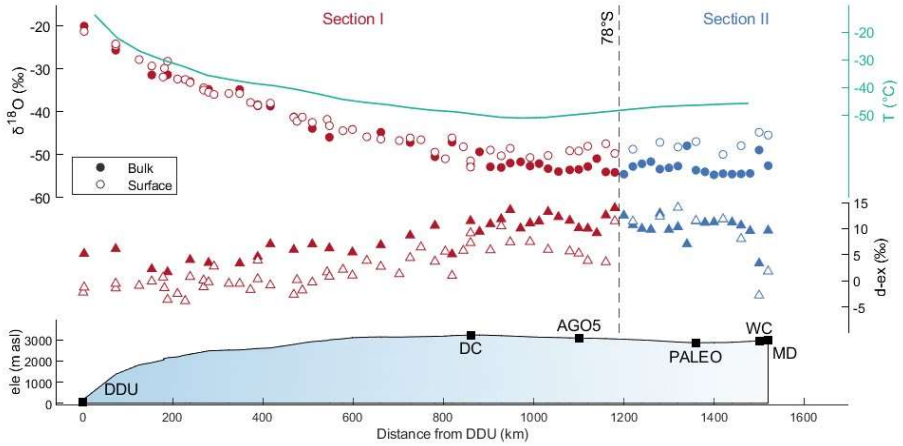

Figure B1. Spatial distribution of $\delta^{18}O$ and *d-excess* values of surface (empty markers) and bulk (filled markers) samples for Section I (red– north of 78°S) and Section II (blue– south of 78°S). Temperature, elevation and distance from DDU are reported.

Appendix C: LMDZ6iso predictions

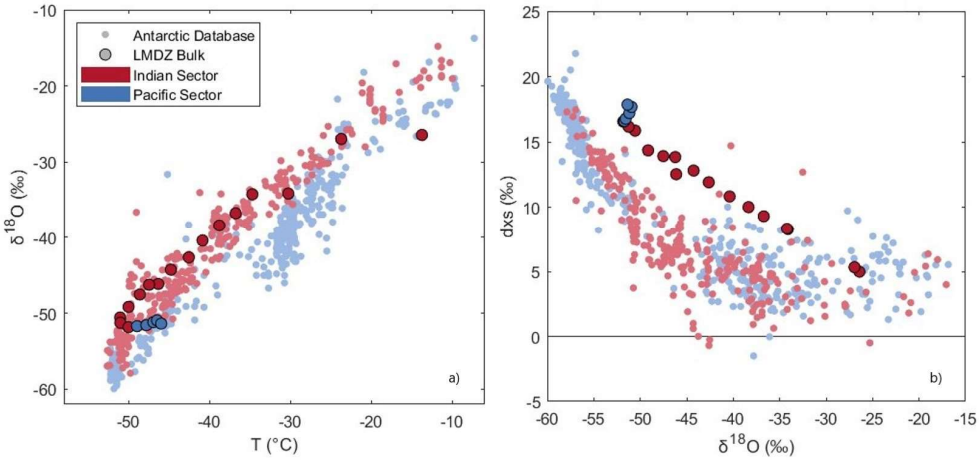

Figure C1. a) δ^{18}O-T relationship and b) *d-excess* vs δ^{18}O for LMDZ6iso bulk samples of the traverse compared to observations from Antarctic database, separated into Pacific and Indian sectors.

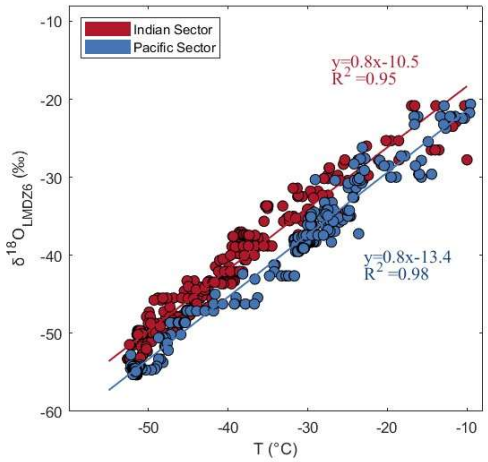

Figure C2. δ^{18}O-T spatial relationship predicted by LMDZ6iso for the Antarctic dataset, separated into Pacific and Indian sectors.

Author contributions

AP and MC performed the measurement in Venice and Paris; AP, CLDS conducted the back-trajectory analysis using the FLEXPART model; AP, ND and CA computed the LMDZ6iso simulations; MC, PDA, JS, AS and MF collected the snow samples during the EAIIST traverse; AP and MC wrote the manuscript draft; AL, ND, PDA, JS, AS, MF and BS reviewed the manuscript.

Competing interests

The authors declare that they have no conflict of interest.

Acknowledgements

The authors would like to thank all the staff of the East International Ice sheet traverse that made possible the collection of the samples used in this manuscript. We also acknowledge all the logistical support received from the PNRA and IPEV for the safe samples handling, storage and transportation. This project received funding from the "Programma Nazionale per la Ricerca in Antartide" ("EAIIST" PNRA16_00049-B and "EAIIST-phase2" PNRA19_00093 projects). The maps were produced using MATLAB (MathWorks Inc.) and its Mapping Toolbox.

Financial support

This work was supported by the Polar Science PhD scholarship from Ca' Foscari University of Venice and the Erasmus+ program. This research has been supported by the European Research Council, Project SAMIR (HORIZON: European Research Council, grant no. 101116660).

References

Baroni, M., Bard, E., Petit, J.-R., Magand, O., Bourlès, D., 2011. Volcanic and solar activity, and atmospheric circulation influences on cosmogenic 10Be fallout at Vostok and Concordia (Antarctica) over the last 60 years. Geochim. Cosmochim. Acta 75, 7132–7145. https://doi.org/10.1016/j.gca.2011.09.002

Beria, H., Larsen, J.R., Ceperley, N.C., Michelon, A., Vennemann, T., Schaefli, B., 2018. Understanding snow hydrological processes through the lens of stable water isotopes. *WIREs Water* 5, e1311. https://doi.org/10.1002/wat2.1311

Bintanja, R., 1998. The contribution of snowdrift sublimation to the surface mass balance of Antarctica. Ann. Glaciol. 27, 251–259. https://doi.org/10.3189/1998AoG27-1-251-259

Boucher, O., Servonnat, J., Albright, A.L., Aumont, O., Balkanski, Y., Bastrikov, V., Bekki, S., Bonnet, R., Bony, S., Bopp, L., Braconnot, P., Brockmann, P., Cadule, P., Caubel, A., Cheruy, F., Codron, F., Cozic, A., Cugnet, D., D'Andrea, F., Davini, P., de Lavergne, C., Denvil, S., Deshayes, J., Devilliers, M., Ducharne, A., Dufresne, J.-L., Dupont, E., Éthé, C., Fairhead, L., Falletti, L., Flavoni, S., Foujols, M.-A., Gardoll, S., Gastineau, G., Ghattas, J., Grandpeix, J.-Y., Guenet, B., Guez, E., Lionel, Guilyardi, E., Guimberteau, M., Hauglustaine, D., Hourdin, F., Idelkadi, A., Joussaume, S., Kageyama, M., Khodri, M., Krinner, G., Lebas, N., Levavasseur, G., Lévy, C., Li, L., Lott, F., Lurton, T., Luyssaert, S., Madec, G., Madeleine, J.-B., Maignan, F., Marchand, M., Marti, O., Mellul, L., Meurdesoif, Y., Mignot, J., Musat, I., Ottlé, C., Peylin, P., Planton, Y., Polcher, J., Rio, C., Rochetin, N., Rousset, C., Sepulchre, P., Sima, A., Swingedouw, D., Thiéblemont, R., Traore, A.K., Vancoppenolle, M., Vial, J., Vialard, J., Viovy, N., Vuichard, N., 2020. Presentation and Evaluation of the IPSL-CM6A-LR Climate Model. J. Adv. Model. Earth Syst. 12, e2019MS002010. https://doi.org/10.1029/2019MS002010

Casado, M., Hébert, R., Faranda, D., Landais, A., 2023. The quandary of detecting the signature of climate change in Antarctica. Nat. Clim. Change 13, 1082–1088. https://doi.org/10.1038/s41558-023-01791-5

Casado, M., Landais, A., Picard, G., Arnaud, L., Dreossi, G., Stenni, B., Prié, F., 2021. Water Isotopic Signature of Surface Snow Metamorphism in Antarctica. Geophys. Res. Lett. 48, e2021GL093382. https://doi.org/10.1029/2021GL093382

Casado, M., Landais, A., Picard, G., Münch, T., Laepple, T., Stenni, B., Dreossi, G., Ekaykin, A., Arnaud, L., Genthon, C., Touzeau, A., Masson-Delmotte, V., Jouzel, J., 2018. Archival processes of the water stable isotope signal in East Antarctic ice cores. The Cryosphere 12, 1745–1766. https://doi.org/10.5194/tc-12-1745-2018

Casado, M., Münch, T., Laepple, T., 2020. Climatic information archived in ice cores: impact of intermittency and diffusion on the recorded isotopic signal in Antarctica. Clim. Past 16, 1581–1598. https://doi.org/10.5194/cp-16-1581-2020

Casado, M., Orsi, A.J., Landais, A., 2017. On the limits of climate reconstruction from water stable isotopes in polar ice cores. Past Glob. Chang. Mag. 25, 146–147. https://doi.org/10.22498/pages.25.3.146

Charles, C.D., Rind, D., Jouzel, J., Koster, R.D., Fairbanks, R.G., 1994. Glacial-interglacial changes in moisture sources for greenland: influences on the ice core record of climate. Science 263, 508–511. https://doi.org/10.1126/science.263.5146.508

Craig and Gordon, 1965. Deuterium and oxygen-18 variations in the ocean and marine atmosphere – ScienceOpen [WWW Document]. URL https://www.scienceopen.com/document?vid=3c68a140-4141-41c0-be2e-90f1e228e8a7 (accessed 1.29.25).

Craig, H., 1961. Standard for Reporting Concentrations of Deuterium and Oxygen-18 in Natural Waters. Science 133, 1833–1834. https://doi.org/10.1126/science.133.3467.1833

Dansgaard, W., 1964. Stable isotopes in precipitation. Tellus B, 16(4), 436–468.

Dietrich, L.J., Steen-Larsen, H., Wahl, S., Jones, T., Town, M., Werner, M., 2023. Snow-Atmosphere Humidity Exchange at the Ice Sheet Surface Alters Annual Mean Climate Signals in Ice Core Records. Geophys. Res. Lett. 50. https://doi.org/10.1029/2023GL104249

Dreossi, G., Masiol, M., Stenni, B., Zannoni, D., Scarchilli, C., Ciardini, V., Casado, M., Landais, A., Werner, M., Cauquoin, A., Casasanta, G., Del Guasta, M., Posocco, V., Barbante, C., 2024. A decade (2008–2017) of water stable isotope composition of precipitation at Concordia Station, East Antarctica. The Cryosphere 18, 3911–3931. https://doi.org/10.5194/tc-18-3911-2024

Dutrievoz, N., Agosta, C., Risi, C., Vignon, É., Nguyen, S., Landais, A., Fourré, E., Leroy-Dos Santos, C., Casado, M., Ollivier, Inès., Jouzel, J., Roche, D., Minster, B., Prié, F., 2025. Antarctic water stable isotopes in the global atmospheric model

LMDZ6: from climatology to boundary layer processes. Presented at the EGU General Assembly Conference Abstracts, p. 19539. https://doi.org/10.5194/egusphere-egu24-19539

Ekaykin, A., Eberlein, L., Lipenkov, V., Popov, S., Scheinert, M., Schröder, L., Turkeev, A., 2016. Non-climatic signal in ice core records: Lessons from Antarctic megadunes. The Cryosphere 10, 1217–1227. https://doi.org/10.5194/tc-10-1217-2016

Ekaykin, A.A., Lipenkov, V.Y., Barkov, N.I., Petit, J.R., Masson-Delmotte, V., 2002. Spatial and temporal variability in isotope composition of recent snow in the vicinity of Vostok station, Antarctica: implications for ice-core record interpretation. Ann. Glaciol. 35, 181–186. https://doi.org/10.3189/172756402781816726

EPICA community members, Augustin, L., Barbante, C., Barnes, P.R.F., Marc Barnola, J., Bigler, M., Castellano, E., Cattani, O., Chappellaz, J., Dahl-Jensen, D., Delmonte, B., Dreyfus, G., Durand, G., Falourd, S., Fischer, H., Flückiger, J., Hansson, M.E., Huybrechts, P., Jugie, G., Johnsen, S.J., Jouzel, J., Kaufmann, P., Kipfstuhl, J., Lambert, F., Lipenkov, V.Y., Littot, G.C., Longinelli, A., Lorrain, R., Maggi, V., Masson-Delmotte, V., Miller, H., Mulvaney, R., Oerlemans, J., Oerter, H., Orombelli, G., Parrenin, F., Peel, D.A., Petit, J.-R., Raynaud, D., Ritz, C., Ruth, U., Schwander, J., Siegenthaler, U., Souchez, R., Stauffer, B., Peder Steffensen, J., Stenni, B., Stocker, T.F., Tabacco, I.E., Udisti, R., van de Wal, R.S.W., van den Broeke, M., Weiss, J., Wilhelms, F., Winther, J.-G., Wolff, E.W., Zucchelli, M., EPICA community members (participants are listed alphabetically), 2004. Eight glacial cycles from an Antarctic ice core. Nature 429, 623–628. https://doi.org/10.1038/nature02599

Eyring, V., Bony, S., Meehl, G.A., Senior, C.A., Stevens, B., Stouffer, R.J., Taylor, K.E., 2016. Overview of the Coupled Model Intercomparison Project Phase 6 (CMIP6) experimental design and organization. Geosci. Model Dev. 9, 1937–1958. https://doi.org/10.5194/gmd-9-1937-2016

Frezzotti, M., Urbini, S., Proposito, M., Scarchilli, C., Gandolfi, S., 2007. Spatial and temporal variability of surface mass balance near Talos Dome, East Antarctica. J. Geophys. Res. Earth Surf. 112, F02032. https://doi.org/10.1029/2006JF000638

Goursaud, S., Masson-Delmotte, V., Favier, V., Orsi, A., Werner, M., 2018. Water stable isotope spatio-temporal variability in Antarctica in 1960–2013: observations and simulations from the ECHAM5-wiso atmospheric general circulation model. Clim. Past 14, 923–946. https://doi.org/10.5194/cp-14-923-2018

Grazioli, J., Madeleine, J.-B., Gallée, H., Forbes, R.M., Genthon, C., Krinner, G., Berne, A., 2017. Katabatic winds diminish precipitation contribution to the Antarctic ice mass balance. Proc. Natl. Acad. Sci. 114, 10858–10863. https://doi.org/10.1073/pnas.1707633114

Helsen, M.M., Van De Wal, R.S.W., Van Den Broeke, M.R., 2007. The Isotopic Composition of Present-Day Antarctic Snow in a Lagrangian Atmospheric Simulation*. J. Clim. 20, 739–756. https://doi.org/10.1175/JCLI4027.1

Hersbach, H., Bell, B., Berrisford, P., Hirahara, S., Horányi, A., Muñoz-Sabater, J., Nicolas, J., Peubey, C., Radu, R., Schepers, D., Simmons, A., Soci, C., Abdalla, S., Abellan, X., Balsamo, G., Bechtold, P., Biavati, G., Bidlot, J., Bonavita, M., De Chiara, G., Dahlgren, P., Dee, D., Diamantakis, M., Dragani, R., Flemming, J., Forbes, R., Fuentes, M., Geer, A., Haimberger, L., Healy, S., Hogan, R.J., Hólm, E., Janisková, M., Keeley, S., Laloyaux, P., Lopez, P., Lupu, C., Radnoti, G., de Rosnay, P., Rozum, I., Vamborg, F., Villaume, S., Thépaut, J.-N., 2020. The ERA5 global reanalysis. Q. J. R. Meteorol. Soc. 146, 1999–2049. https://doi.org/10.1002/qj.3803

Hirsch, N., Zuhr, A., Münch, T., Hörhold, M., Freitag, J., Dallmayr, R., Laepple, T., 2023. Stratigraphic noise and its potential drivers across the plateau of Dronning Maud Land, East Antarctica. The Cryosphere 17, 4207–4221. https://doi.org/10.5194/tc-17-4207-2023

Hourdin, F., Ferster, B., Deshayes, J., Mignot, J., Musat, I., Williamson, D., 2023. Toward machine-assisted tuning avoiding the underestimation of uncertainty in climate change projections. Sci. Adv. 9, eadf2758. https://doi.org/10.1126/sciadv.adf2758

Hourdin, F., Rio, C., Grandpeix, J.-Y., Madeleine, J.-B., Cheruy, F., Rochetin, N., Jam, A., Musat, I., Idelkadi, A., Fairhead, L., Foujols, M.-A., Mellul, L., Traore, A.-K., Dufresne, J.-L., Boucher, O., Lefebvre, M.-P., Millour, E., Vignon, E., Jouhaud, J., Diallo, F.B., Lott, F., Gastineau, G., Caubel, A., Meurdesoif, Y., Ghattas, J., 2020. LMDZ6A: The Atmospheric Component of the IPSL Climate Model With Improved and Better Tuned Physics. J. Adv. Model. Earth Syst. 12, e2019MS001892. https://doi.org/10.1029/2019MS001892

Hughes, A.G., Wahl, S., Jones, T.R., Zuhr, A., Hörhold, M., White, J.W.C., Steen-Larsen, H.C., 2021. The role of sublimation as a driver of climate signals in the water isotope content of surface snow: laboratory and field experimental results. The Cryosphere 15, 4949–4974. https://doi.org/10.5194/tc-15-4949-2021

Jouzel, J., Masson-Delmotte, V., Cattani, O., Dreyfus, G., Falourd, S., Hoffmann, G., Minster, B., Nouet, J., Barnola, J.M., Chappellaz, J., Fischer, H., Gallet, J.C., Johnsen, S., Leuenberger, M., Loulergue, L., Luethi, D., Oerter, H., Parrenin, F., Raisbeck, G., Raynaud, D., Schilt, A., Schwander, J., Selmo, E., Souchez, R., Spahni, R., Stauffer, B., Steffensen, J.P., Stenni, B., Stocker, T.F., Tison, J.L., Werner, M., and Wolff, E.W., 2007. Orbital and millennial Antarctic climate variability over the past 800,000 years. Science 317(5839), 793–796.

Jouzel, J., Vimeux, F., Caillon, N., Delaygue, G., Hoffmann, G., Masson-Delmotte, V., and Parrenin, F., 2003. Magnitude of isotope/temperature scaling for interpretation of central Antarctic ice cores. Journal of Geophysical Research: Atmospheres 108(D12).

Jouzel, J., Alley, R.B., Cuffey, K.M., Dansgaard, W., Grootes, P., Hoffmann, G., Johnsen, S.J., Koster, R.D., Peel, D., Shuman, C.A., Stievenard, M., Stuiver, M., and White, J., 1997. Validity of the temperature reconstruction from water isotopes in ice cores. Journal of Geophysical Research: Oceans 102(C12), 26471–26487.

Laepple, T., Münch, T., Casado, M., Hoerhold, M., Landais, A., Kipfstuhl, S., 2018. On the similarity and apparent cycles of isotopic variations in East Antarctic snow pits. The Cryosphere 12, 169–187. https://doi.org/10.5194/tc-12-169-2018

Landais, A., Casado, M., Prié, F., Magand, O., Arnaud, L., Ekaykin, A., Petit, J.-R., Picard, G., Fily, M., Minster, B., Touzeau, A., Goursaud, S., Masson-Delmotte, V., Jouzel, J., Orsi, A., 2017. Surface studies of water isotopes in Antarctica for quantitative interpretation of deep ice core data. Comptes Rendus Geosci. 349, 139–150. https://doi.org/10.1016/j.crte.2017.05.003

Lilien, D.A., Steinhage, D., Taylor, D., Parrenin, F., Ritz, C., Mulvaney, R., Martín, C., Yan, J.-B., O'Neill, C., Frezzotti, M., Miller, H., Gogineni, P., Dahl-Jensen, D., Eisen, O., 2021. Brief communication: New radar constraints support presence of ice older than 1.5 Myr at Little Dome C. The Cryosphere 15, 1881–1888. https://doi.org/10.5194/tc-15-1881-2021

Lorius, C., Merlivat, L., and Hagemann, R., 1969. Variation in the mean deuterium content of precipitations in Antarctica. Journal of Geophysical Research 74(28), 7027–7031.

Lorius, C., Merlivat, L., 1977. Distribution of mean surface stable isotope values in East Antarctica: Observed changes with depth in the coastal area. Isot. Impurities Snow Ice 118, 127–137.

Ma, T., Li, L., Li, Y., An, C., Yu, J., Ma, H., Jiang, S., Shi, G., 2020. Stable isotopic composition in snowpack along the traverse from a coastal location to Dome A (East Antarctica): Results from observations and numerical modeling. Polar Sci. 24, 100510. https://doi.org/10.1016/j.polar.2020.100510

Masson-Delmotte, V., Buiron, D., Ekaykin, A., Frezzotti, M., Gallée, H., Jouzel, J., Krinner, G., Landais, A., Motoyama, H., Oerter, H., Pol, K., Pollard, D., Ritz, C., Schlosser, E., Sime, L.C., Sodemann, H., Stenni, B., Uemura, R., Vimeux, F., 2011. A comparison of the present and last interglacial periods in six Antarctic ice cores. Clim. Past 7, 397–423. https://doi.org/10.5194/cp-7-397-2011

Masson-Delmotte, V., Hou, S., Ekaykin, A., Jouzel, J., Aristarain, A., Bernardo, R.T., Bromwich, D., Cattani, O., Delmotte, M., Falourd, S., Frezzotti, M., Gallée, H., Genoni, L., Isaksson, E., Landais, A., Helsen, M.M., Hoffmann, G., Lopez, J., Morgan, V., Motoyama, H., Noone, D., Oerter, H., Petit, J.R., Royer, A., Uemura, R., Schmidt, G.A., Schlosser, E., Simões, J.C., Steig, E.J., Stenni, B., Stievenard, M., van den Broeke, M.R., van de Wal, R.S.W., van de Berg, W.J., Vimeux, F., White, J.W.C., 2008. A Review of Antarctic Surface Snow Isotopic Composition: Observations, Atmospheric Circulation, and Isotopic Modeling*. J. Clim. 21, 3359–3387. https://doi.org/10.1175/2007JCLI2139.1

Masson-Delmotte, V., Jouzel, J., Landais, A., Stievenard, M., Johnsen, S.J., White, J.W.C., Werner, M., Sveinbjornsdottir, A., Fuhrer, K., 2005. GRIP deuterium excess reveals rapid and orbital-scale changes in Greenland moisture origin. Science 309, 118–121. https://doi.org/10.1126/science.1108575

Merlivat and Jouzel, 1979. Global climatic interpretation of the deuterium-oxygen 18 relationship for precipitation - Merlivat - 1979 - Journal of Geophysical Research: Oceans - Wiley Online Library [WWW Document]. URL https://agupubs.onlinelibrary.wiley.com/doi/10.1029/JC084iC08p05029 (accessed 1.29.25).

Münch, T., Kipfstuhl, S., Freitag, J., Meyer, H., Laepple, T., 2016. Regional climate signal vs. local noise: a two-dimensional view of water isotopes in Antarctic firn at Kohnen Station, Dronning Maud Land. Clim. Past 12, 1565–1581. https://doi.org/10.5194/cp-12-1565-2016

Münch, T., Werner, M., Laepple, T., 2021. How precipitation intermittency sets an optimal sampling distance for temperature reconstructions from Antarctic ice cores. Clim. Past 17, 1587–1605. https://doi.org/10.5194/cp-17-1587-2021

Neumann, T.A., Waddington, E.D., Steig, E.J., and Grootes, P.M., 2005. Non-climate influences on stable isotopes at Taylor Mouth, Antarctica. Journal of Glaciology 51(173), 248–258.

Ollivier, I., Steen-Larsen, H.C., Stenni, B., Arnaud, L., Casado, M., Cauquoin, A., Dreossi, G., Genthon, C., Minster, B., Picard, G., Werner, M., and Landais, A., 2025. Surface processes and drivers of the snow water stable isotopic composition at Dome C, East Antarctica: A multi-dataset and modelling analysis. *The Cryosphere* 19(1), 173–200.

Ooms, A., Casado, M., Picard, G., Arnaud, L., Hörhold, M., Spolaor, A., Traversi, R., Savarino, J., Ginot, P., Akers, P., Twarloh, B., Masson-Delmotte, V., 2025. Inter-annual snow accumulation and meter-scale variability from trench measurements at Dome C, Antarctica. *EGUsphere* 2025, 1–39. https://doi.org/10.5194/egusphere-2025-3259

Parrenin, F., Cavitte, M.G.P., Blankenship, D.D., Chappellaz, J., Fischer, H., Gagliardini, O., Masson-Delmotte, V., Passalacqua, O., Ritz, C., Roberts, J., Siegert, M.J., Young, D.A., 2017. Is there 1.5-million-year-old ice near Dome C, Antarctica? The Cryosphere 11, 2427–2437. https://doi.org/10.5194/tc-11-2427-2017

Petit, J.R., Jouzel, J., Pourchet, M., and Merlivat, L., 1982. A detailed study of snow accumulation and stable isotope content in Dome C (Antarctica). *Journal of Geophysical Research: Oceans* 87(C6), 4301–4308.

Petit, J.R., White, J.W.C., Young, N.W., Jouzel, J., and Korotkevich, Y.S., 1991. Deuterium excess in recent Antarctic snow. *Journal of Geophysical Research: Atmospheres* 96(D3), 5113–5122.Reijmer, C.H., Broeke, M.R. van den, Scheele, M.P., 2002. Air Parcel Trajectories and Snowfall Related to Five Deep Drilling Locations in Antarctica Based on the ERA-15 Dataset.

Petteni, A., Fourré, E., Gautier, E., Spagnesi, A., Jacob, R., Akers, P.D., Zannoni, D., Gabrieli, J., Jossoud, O., Prié, F., Landais, A., Tcheng, T., Stenni, B., Savarino, J., Ginot, P., Casado, M., 2025. Interlaboratory comparison of continuous flow analysis (CFA) systems for high-resolution water isotope measurements in ice cores. *Atmospheric Measurement Techniques* 18, 5435–5455. https://doi.org/10.5194/amt-18-5435-2025

Reijmer, C.H., Van den Broeke, M.R., and Scheele, M.P., 2002. Air parcel trajectories and snowfall related to five deep drilling locations in Antarctica based on the ERA-15 dataset. *Journal of Climate* 15(14), 1957–1968.

Risi, C., Noone, D., Frankenberg, C., and Worden, J., 2013. Role of continental recycling in intraseasonal variations of continental moisture as deduced from model simulations and water vapor isotopic measurements. *Water Resources Research* 49(7), 4136–4156.

Risi, C., Bony, S., Vimeux, F., Jouzel, J., 2010. Water-stable isotopes in the LMDZ4 general circulation model: Model evaluation for present-day and past climates and applications to climatic interpretations of tropical isotopic records. J. Geophys. Res. Atmospheres 115. https://doi.org/10.1029/2009JD013255

Roussel, M.-L., Lemonnier, F., Genthon, C., and Krinner, G., 2020. Brief communication: Evaluating Antarctic precipitation in ERA5 and CMIP6 against CloudSat observations. The Cryosphere 14, 2715–2727. https://doi.org/10.5194/tc-14-2715-2020

Scarchilli, C., Frezzotti, M., Grigioni, P., De Silvestri, L., Agnoletto, L., Dolci, S., 2010. Extraordinary blowing snow transport events in East Antarctica. Clim. Dyn. 34, 1195–1206. https://doi.org/10.1007/s00382-009-0601-4

Scarchilli, C., Frezzotti, M., Ruti, P., 2011. Snow precipitation at four ice core sites in East Antarctica: Provenance, seasonality and blocking factors. Clim. Dyn. 37, 2107–2125. https://doi.org/10.1007/s00382-010-0946-4

Schlosser, E., Reijmer, C., Oerter, H., Graf, W., 2004. The influence of precipitation origin on the δ18O–T relationship at Neumayer station, Ekstrmisen, Antarctica. Ann. Glaciol. 39, 41–48. https://doi.org/10.3189/172756404781814276

Sime, L.C., Tindall, J.C., Wolff, E.W., Connolley, W.M., Valdes, P.J., 2008. Antarctic isotopic thermometer during a CO_2-forced warming event. Clim. Dyn. 31, 813–826. https://doi.org/10.1029/2008JD010395

Sodemann, H., Stohl, A., 2009. Asymmetries in the moisture origin of Antarctic precipitation. Geophys. Res. Lett. 36, L22803. https://doi.org/10.1029/2009GL040242

Steen-Larsen, H.C., Sveinbjörnsdottir, A.E., Peters, A.J., Masson-Delmotte, V., Guishard, M.P., Hsiao, G., Jouzel, J., Noone, D., Warren, J.K., White, J.W.C., 2014. Climatic controls on water vapor deuterium excess in the marine boundary layer of the North Atlantic based on 500 days of in situ, continuous measurements. Atmospheric Chem. Phys. 14, 7741–7756. https://doi.org/10.5194/acp-14-7741-2014

Stenni, B., Scarchilli, C., Masson-Delmotte, V., Schlosser, E., Ciardini, V., Dreossi, G., Grigioni, P., Bonazza, M., Cagnati, A., Karlicek, D., Risi, C., Udisti, R., Valt, M., 2016. Three-year monitoring of stable isotopes of precipitation at ConcordiaStation, East Antarctica. The Cryosphere 10, 2415–2428. https://doi.org/10.5194/tc-10-2415-2016

Touzeau, A., Landais, A., Stenni, B., Uemura, R., Fukui, K., Fujita, S., Guilbaud, S., Ekaykin, A., Casado, M., Barkan, E., Luz, B., Magand, O., Teste, G., Le Meur, E., Baroni, M., Savarino, J., Bourgeois, I., Risi, C., 2016. Acquisition of isotopic composition for surface snow in East Antarctica and the links to climatic parameters. The Cryosphere 10, 837–852. https://doi.org/10.5194/tc-10-837-2016

Traversa, G., Fugazza, D., Frezzotti, M., 2023. Megadunes in Antarctica: migration and characterization from remote and in situ observations. The Cryosphere 17, 427–444. https://doi.org/10.5194/tc-17-427-2023

Uemura, R., Masson-Delmotte, V., Jouzel, J., Landais, A., Motoyama, H., Stenni, B., 2012. Ranges of moisture-source temperature estimated from Antarctic ice cores stable isotope records over glacial–interglacial cycles. Clim. Past 8, 1109–1125. https://doi.org/10.5194/cp-8-1109-2012

Vimeux, F., Masson, V., Jouzel, J., Stievenard, M., and Petit, J.R., 1999. Glacial–interglacial changes in ocean surface conditions in the Southern Hemisphere. Nature 398(6726), 410–413.

Wahl, S., Steen-Larsen, H.C., Hughes, A.G., Dietrich, L.J., Zuhr, A., Behrens, M., Faber, A.-K., Hörhold, M., 2022. Atmosphere-Snow Exchange Explains Surface Snow Isotope Variability. Geophys. Res. Lett. 49, e2022GL099529. https://doi.org/10.1029/2022GL099529

Werner, M., Langebroek, P.M., Carlsen, T., Herold, M., Lohmann, G., 2011. Stable water isotopes in the ECHAM5 general circulation model: Toward high-resolution isotope modeling on a global scale. https://doi.org/10.1029/2011JD015681

Xiao, C., Ding, M., Masson-Delmotte, V., Zhang, R., Jin, B., Ren, J., Li, C., Werner, M., Wang, Y., Cui, X., Wang, X., 2013. Stable isotopes in surface snow along a traverse route from Zhongshan station to Dome A, East Antarctica. Clim. Dyn. 41, 2427–2438. https://doi.org/10.1007/s00382-012-1580-0